Robot Path Planning for Material Deposition and Metrology in Hybrid Manufacturing

A Thesis Presented for the

Master of Science

Degree

The University of Tennessee, Knoxville

Tiffany Quigley

December 2022

Copyright © 2022 by Tiffany Quigley
All rights reserved.

Acknowledgements

I would like to thank Dr. Jared and Dr. Hamel for providing me with the opportunity to expand my knowledge in a hands-on environment. I have truly learned more in the last year of working in the lab than I have in any classroom. Thank you to Devon Goodspeed for always being willing to stay late to help finish an experiment and reviewing countless presentations and papers. I would also like to express my gratitude to Joshua Penney, Tim No, and Aaron Cornelius for their support and taking the time to teach me the skills required for this thesis to be successful. Thank you to my committee members for taking the time to review and advise on this thesis.

Abstract

Current methods of manufacturing large scale parts can take up to six months to generate the objective product. The objective of the wire arc additive manufacturing (WAAM) hybrid cell is to significantly reduce lead time associated with large scale parts. The WAAM process utilizes a 6 degree-of-freedom (DOF) robot manipulator in addition to a 2 DOF part positioner. 5 degrees of freedom are necessary for an effective WAAM process, leaving 3 DOF as redundant in this cell. This thesis serves to prove successful implementation of redundant kinematics on a WAAM robotic system. This is accomplished by maintaining a gravity aligned welding torch. Maintaining gravity alignment means the welding torch remains in vertical alignment to the initial substrate in which it is printing on in a 1 G configuration. Gravity alignment is demonstrated in both simulation and real prints during the WAAM process of the hybrid manufacturing cell. After printing, the part is translated into position for scanning to inform the subtractive manufacturing process. Scanning in a manual setting can be a long and arduous process to generate scans of sufficient quality for the basis of informed machining. Effective path planning for scanning with the intent to reduce scanning time, increase quality of scans, and move toward a full automation of the hybrid manufacturing cell is also investigated in this thesis. Simulation software is used to create and verify path plans prior to importing and implementing on a 6 DOF robotic manipulator to which a GOM ATOS Q 3D scanner is mounted. The quality, amount of time necessary to produce, and number of scans required to produce a sufficient representation for machining are compared using three methods. The first method is a manual scanning configuration, the second is using a generalized path plan, and the third is using a geometry-based path plan.

Table of Contents

Chapter 1 1
Introduction 1
Chapter 2 4
Background 4
2.1 Wire Arc Additive Manufacturing (WAAM) 4
2.2 Hybrid Manufacturing 4
2.3 GOM Scanner Background 5
2.3.1 Blue light Fringe Projection Scanning 5
2.4 UT Hybrid Cell 7
Chapter 3 12
Path Planning Redundant DOF Robotic Manipulation for Wire Arc Additive Manufacturing 12
3.1 Welding Parameter Development for Path Planning Process 12
3.1.1 Bead height 12
3.1.2 Wire diameter 12
3.1.3 Wait Time Between Layers 13
3.1.4 Contact Tip to Workpiece Distance 13
3.1.5 Geometry Complications 15
3.1.6 Starts and Stops 16
3.1.7 Heat 17
3.2 Path Planning 18
3.2.1 Slicing 19
3.2.2 Importing Contours into MATLAB 21
3.2.3 Importing Path into Octopuz 24
3.2.4 Path Plan on Robot 25
3.2.5 Coupling of the Part Positioner 27
Chapter 4 32
Mounting of Scanner to Robot 32

4.1 Hardware Design 32
4.2 Straight vs. 90 degree Configuration 33
4.2.1 Kinematics 33
4.2.2 Collision Avoidance 35
4.3 GOM Software 36
4.3.1 Sufficient Reference Points 36
4.3.2 Field of View 37
4.3.3 Scan Result Using KR250 37
Chapter 5 40
Path Planning for Scanning 40
5.1 Motivation 40
5.2 Static Configuration Scanning 40
5.2.1 Static Configuration Camera Straight Down 40
5.2.2 Implementing 25-Degree Mounting Angle 43
5.3 Scanning View Constraint Study 45
5.4 Generalized Path Plan for Scanning 49
5.5 Geometry Based Path Planning for Scanning 52
5.5.1 Surfacing Function 53
5.5.2 Utilization of the Path Planner 54
5.5.3 Refinement of the Path Planner for Scanning 57
5.6 Data Comparison/Results 61
5.6.1 Static Configuration Results 62
5.6.2 Generalized Path Plan Results 63
5.6.3 Comparisons 64
5.7 Challenges 68
5.7.1 Transformation Error 68
5.7.2 Measurement Delay 69
5.7.3 Not Enough Reference Points 70
Chapter 6 72
Conclusions And Recommendations 72

6.1 Conclusions 72
6.2 Recommendations 72
6.2.1 Implementation of Algorithm 72
6.2.2 Coupling of the KR250 73
Bibliography 74

List of Tables

Table 1: Comparison of Joint Axis Positions Between Simulation and Actual 26
Table 2: Comparison of Scan Results 66

List of Figures

Figure 1: RP-1 CAD Model 2
Figure 2: RP-2 CAD Model 2
Figure 3: AXWJ CAD Model 3
Figure 4: GOM ATOS Q 3D Scanner (Products: ATOS Q, 2022) 5
Figure 5: Triangulation of Blue Light Fringe Projection Scanning (Triangulation: proven measuring principle with a future, 2022) 6
Figure 6: Blue Light Fringe Projection Scanning Depiction (Triangulation: proven measuring principle with a future, 2022) 7
Figure 7: Additive Manufacturing via KR50(left) and KL4000(part positioner) 8
Figure 8: Post Printing Scanning 9
Figure 9: Post-Printing Scan Comparison for Informed Machining 10
Figure 10: Post-Machining Comparison to Desired Geometry 11
Figure 11: Welded Contact Tip 14
Figure 12: Shielding Gas Effects on Hexagon Build 15
Figure 13: Warped Welds Around Turns 16
Figure 14: Graphical Depiction of Start and Stop Position 17
Figure 15: Base Plate Deformation 18
Figure 16: WAAM Path Planning Structure 19
Figure 17: CAD Model Of Desired Geometry 20
Figure 18: Cylinder Fitted, Creation of Slices 20
Figure 19: Slices Generated 21
Figure 20: MATLAB Path Script 23
Figure 21: Graphical User Interface 24
Figure 22: Path Plan Simulation 25
Figure 23: Joint Position Comparison Between Simulation and Actual 26
Figure 24: Kinematic Chain of Robot Mounted to Linear Track (KUKA Robotics, 2017) 28

Figure 25: Robot and Part Positioner Kinematic Chain (KUKA Robotics, 2017) 29
Figure 26: Offset between KR50 and Part Positioner 30
Figure 27: Denavit-Hartenberg System Containing KR50 and KPL3 31
Figure 28: GOM Scanner Mounting Bracket 33
Figure 29: Scanner Mounted in 90 Degree Configuration 34
Figure 30: Scanner Mounted In Line With End Effector 35
Figure 31: Collision in Straight Scanner Configuration 36
Figure 32: Scan Volume 37
Figure 33: Scanning via R250 38
Figure 34: Scan Results of Hexagon Using KR250 39
Figure 35: Hexagon Scan Image Map Using KR250 39
Figure 36: Static Configuration Mount for Scanner 41
Figure 37: Static Configuration of GOM ATOS Q Scanner 42
Figure 38: Result of Scanning in Static Configuration 43
Figure 39: 25-degree Scanner Mounting Angle 44
Figure 40: Scan Results of 25-Degree Configuration 45
Figure 41: Gage Ball Study 46
Figure 42: Schematic Description of Data Analysis Conducted 47
Figure 43: Single Scan Data Set 48
Figure 44: Camera Angle in Relation to Geometry Surface Vs. Error 49
Figure 45: Generalized Path Plan 50
Figure 46: Generalized Scanning Path Plan Image Map 51
Figure 47: Result of Generalized Scanning Path Plan 52
Figure 48: Surfacing Function for Path Planning 53
Figure 49: Surface Based Path Plan 54
Figure 50: Imported Path Plan Orientation Collison 56
Figure 51: Imported Path Plan Orientation Adjustment 56
Figure 52: Surface Nominals along Desired Geometry 57
Figure 53: Nominal Vector Reduction 58
Figure 54: Scanning Path Plan 59

Figure 55: MATLAB Code for Scanning Path Plan 60
Figure 56: Geometry Based Path Plan Using Reference Points 61
Figure 57: Static Configuration Color Map 62
Figure 58: 25-Degree Configuration Color Map 63
Figure 59: Color Map Comparison of Generalized Path Plan (Side View) 64
Figure 60: Data Comparison of Static Configuration, 25-Degree Configuration, and Generalized Path Plan 66
Figure 61: Comparison of Scan Results (Side View) 68
Figure 62: Transformation Error 69
Figure 63: Measurement Delay Screen 70
Figure 64: Insufficient Reference Points Error 71

Chapter 1

Introduction

In comparison to other manufacturing methods, wire arc additive manufacturing (WAAM) diminishes print time, wasted material, and allows for production of more complex geometries. Robotic manipulators are usually implemented into this process by mounting a MIG welding torch as an end effector of the robot and the optional addition of a 2 DOF part positioner. In the hybrid cell used to implement and test the premise of this thesis, WAAM is performed via a 6 DOF robotic manipulator with the welding torch as an end effector, and a 2 DOF part positioner. When using the part positioner in conjunction with the robotic manipulator, some degrees of freedom become redundant. Redundancy in degrees of freedom simply means that the number of degrees of freedom required to define the position of the end-effector in operational space than that required to define the position of the robot in joint space. Configuration of the robot can be optimized for its intended purpose by solving the redundant DOFs. Previous work from Ethan Vals (Vals, 2022) on kinematically solving DOF redundancy for selective geometry applications provided a foundation to expand and refine. Upon integration of the robotic system of the hybrid cell for the purposes of WAAM, a new configuration was created by KUKA to programmatically integrate the part positioner and the linear track it is mounted on into one cohesive unit titled KPL3. The KPL3 was then coupled to the robotic manipulator used for WAAM to maintain gravity alignment where possible in the welding process. Coupling of the systems eased the process of path planning using redundant degrees of freedom. A series of geometries were demonstrated in the process of making this path planning process successful. In conjunction with a funded research project, RP-1, RP-2, and AXWJ-2 were administered for the purpose of printing using WAAM on the hybrid manufacturing cell. AXWJ-2 (Tan, 2015) is designed for axial flow waterjet pump, with RP-1 and RP-2 intended to be incrementally less complex variations.

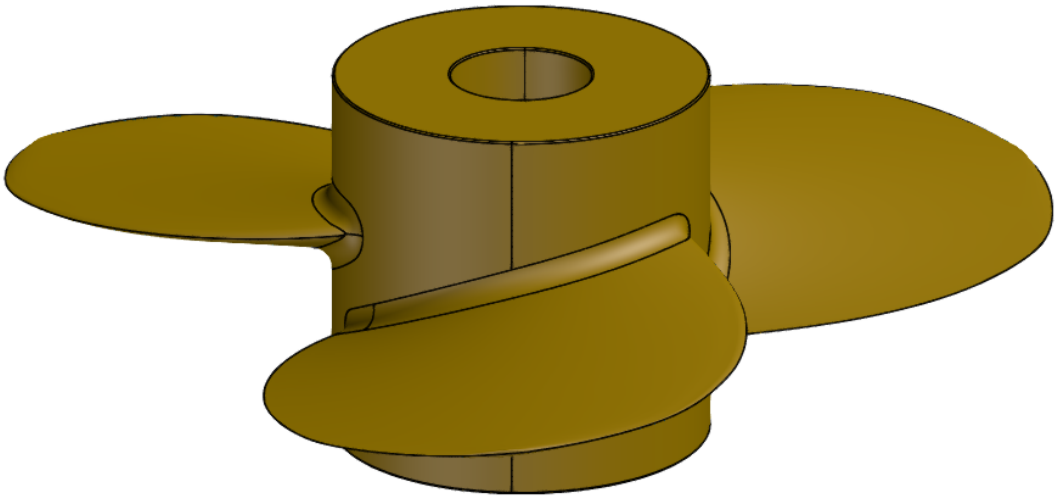


Figure 1: RP-1 CAD Model

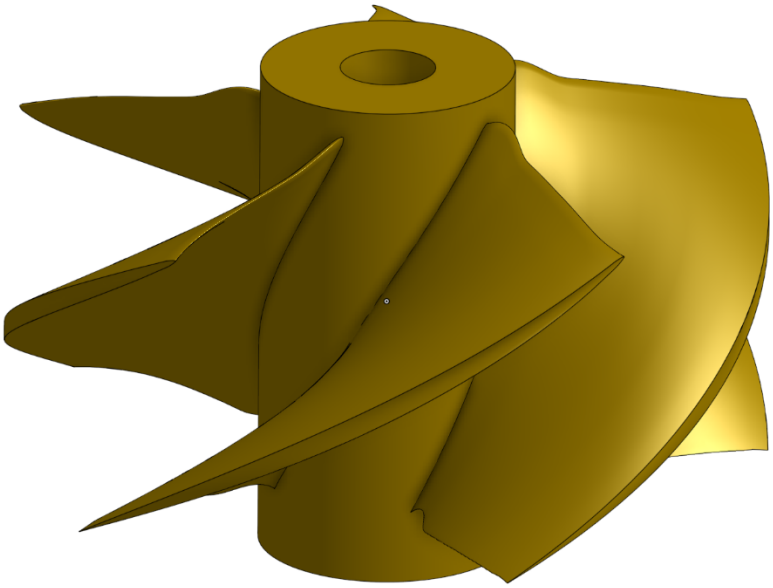


Figure 2: RP-2 CAD Model

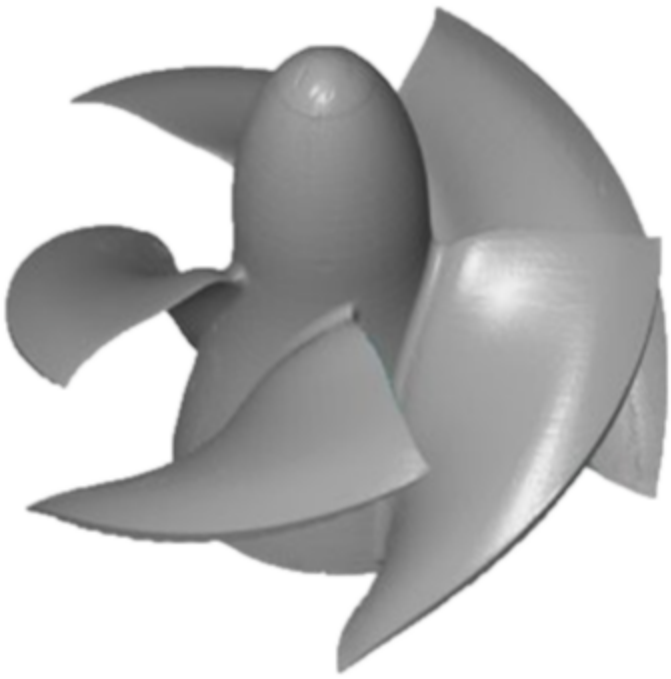


Figure 3: AXWJ CAD Model

Integrating metrology into the hybrid cell allows for informed machining, but as previously mentioned can significantly lengthen the lead time on producing a part. Transitioning metrology into an automated process significantly reduces lead time of the hybrid cell but faces challenges as complexity of parts increase. Upon first mounting the scanner to the KR250, a 6 DOF robotic manipulator, scans were administered to a standard part to prove functionality. It was discovered images of sufficient quality for machining were not only easier to achieve but were also accomplished in less time and with less scans necessary. Quantitative data analysis of a single scan was used to determine ideal scanning configurations and constraints able to be applicable to generating geometry-based path plans for the robotic manipulator.

Chapter 2

Background

2.1 Wire Arc Additive Manufacturing (WAAM)

Wire Arc Additive Manufacturing is direct energy deposition (DED) method of manufacturing in which metal inert gas (MIG) welding is used to deposit layers of material onto an initial substrate. MIG welding is the process of feeding wire into a molten weld pool. This process is done repetitively until a near net shape is created. Incorporating a robotic manipulator into this process allows for diminished manufacturing time, increased part complexity, and more maneuverability. The robotic manipulator used in this process utilizes a Gas Metal Arc Welding (GMAW) power supply with the MIG torch mounted to the end-effector. The part positioner is coupled to the robotic manipulator to easily maneuver the part to best keep the torch gravity aligned, or aligned vertically in relation to the part.

2.2 Hybrid Manufacturing

Hybrid manufacturing encompasses a combination of additive and subtractive manufacturing. The near net shape produced via wire arc additive manufacturing is refined via machining to produce the final product. Creation of a near net shape creates less waste than conventional subtractive machining by producing a geometry of similar shape and size of the desired result via additive manufacturing and then refining via machining. Integrating informed metrology via a 3D scanner into this process makes it possible to determine areas in need of machining or additional deposition. This process is accomplished by scanning the part after printing and comparing the scan generated to a CAD model of the intended geometry. The part is also scanned after machining and compared once more to the intended geometry for iterative refinement.

2.3 GOM Scanner Background

The GOM ATOS Q scanner (Figure 4) is used in this hybrid manufacturing cell to scan the part both post printing and post machining. This scanner is specifically tailored for the scanning of additively manufactured parts. The scanner has a working distance of 490mm and a measuring area range of 100mm x 70mm to 500mm x 370mm which permits reasonable visibility within the hybrid cell with proper manipulation. The scanner uses 8 million points per scan, LED lights for fringe projection, and automatically filters ambient light. It is also capable of triple scan, where 3 scans are administered at variable resolution and compared. 10 meters of fiber optic cable connects the scanner to its power source which accommodates maneuverability of the scanner into ideal scanning configurations.



Figure 4: GOM ATOS Q 3D Scanner (Products: ATOS Q, 2022)

2.3.1 Blue light Fringe Projection Scanning

Blue light fringe projection scanning works by projecting narrow patterns of blue light along the surface of the subject of the scan and is captured by the two cameras. The projector and cameras are at known angles and distances to one another so the image captured can use the pattern of light to triangulate and produce a point cloud replicating the distortions detected in the fringe pattern.

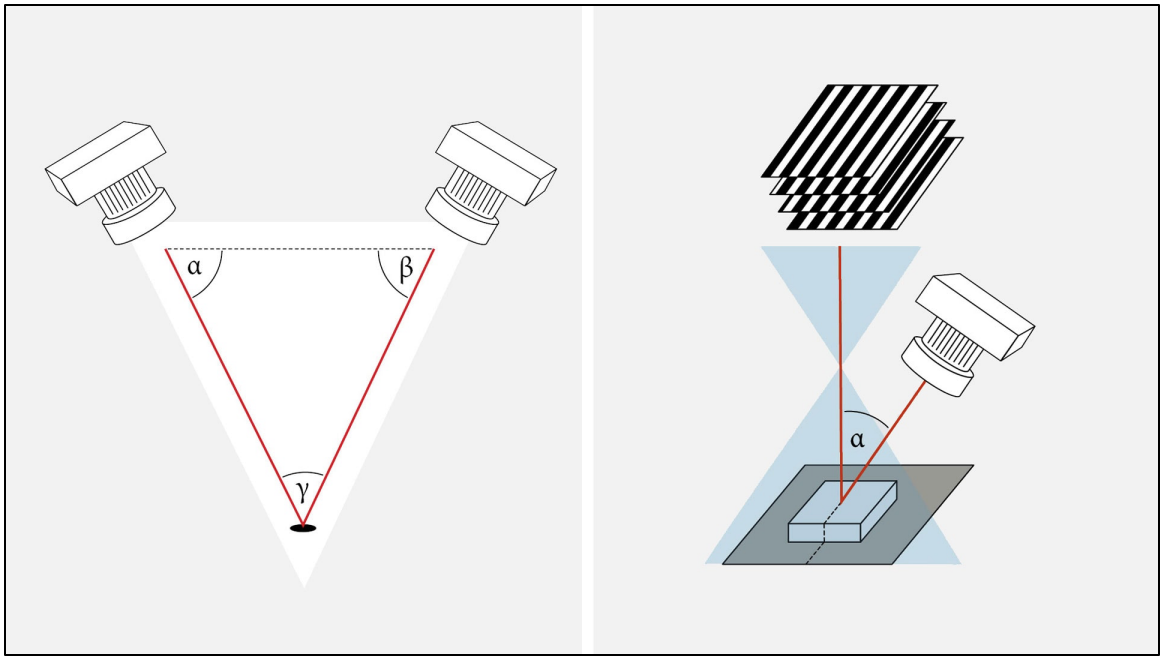


Figure 5: Triangulation of Blue Light Fringe Projection Scanning (Triangulation: proven measuring principle with a future, 2022)

Each scan-generated point cloud is stitched together to create a mesh that replicates the surface of the object being scanned. Once enough scans are taken to generate an acceptable representation of the geometry, the part is polygonized. This is where the total mesh or point cloud generated is transformed into a series of polygons that are stitched together to create one cohesive representation of the geometry. This cohesive unit may be

exported as a CAD model, which is the case for informed machining.

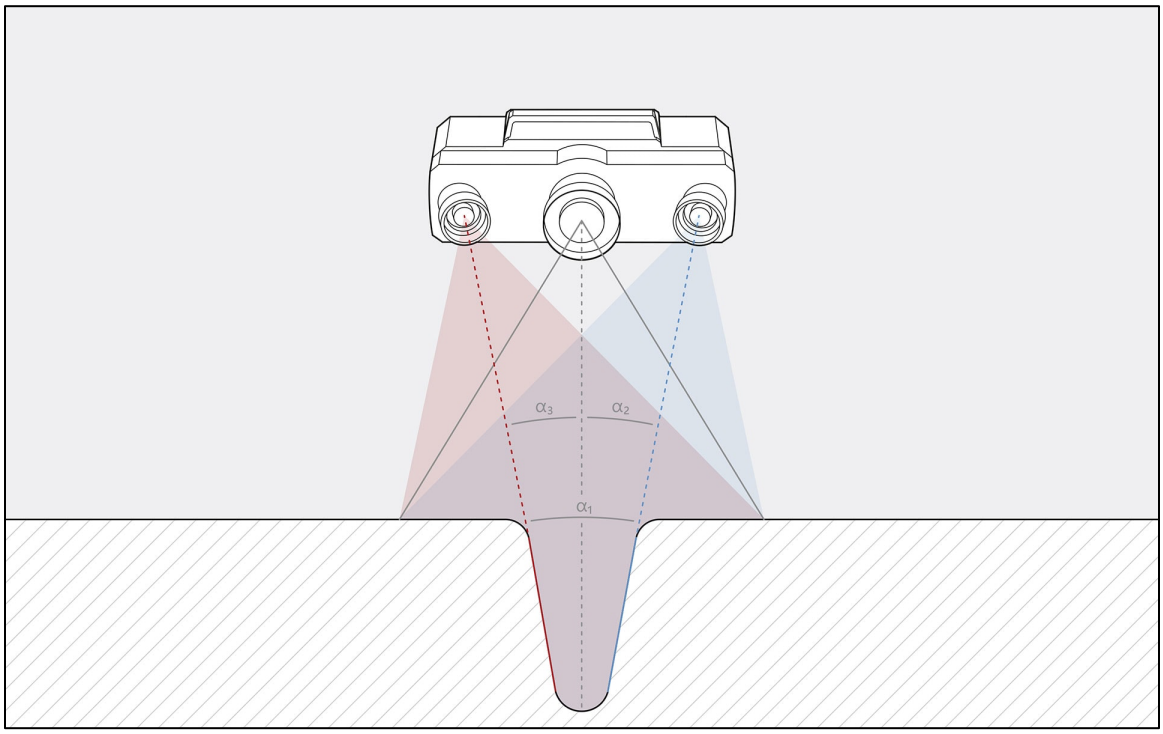


Figure 6: Blue Light Fringe Projection Scanning Depiction (Triangulation: proven measuring principle with a future, 2022)

2.4 UT Hybrid Cell

The hybrid manufacturing cell used for this project consists of two KUKA 6 DOF robotic manipulators, a KL4000 2 DOF part positioner mounted to a linear track, a HAAS 5 axis milling machine, and a GOM ATOS Q 3D scanner. The process begins with wire arc additive manufacturing via a KUKA KR50 6 DOF robotic manipulator with welding torch end effector which welds the imported path plan onto a hub or baseplate mounted to the coupled part positioner (Figure 7).



Figure 7: Additive Manufacturing via KR50(left) and KL4000(part positioner)

Post printing, the part is translated via the linear track into position for scanning (Figure 8). Scans are administered via a GOM ATOS Q fringe projection scanner and polygonized into one cohesive image. After scanning, the part is transported from the linear track robot into the milling machine via the 6 DOF KUKA KR250 robotic manipulator. Scans of the geometry post printing are compared to a CAD model of the desired product and used to inform the subtractive manufacturing process of areas of excess material in need of machining. After machining, the part is returned to the linear track and translated into position for additional scanning. Scans administered post machining are polygonized and compared once again to a CAD model of the desired geometry. This comparison (Figure 10) determines underbuilt areas where additional deposition may be required.

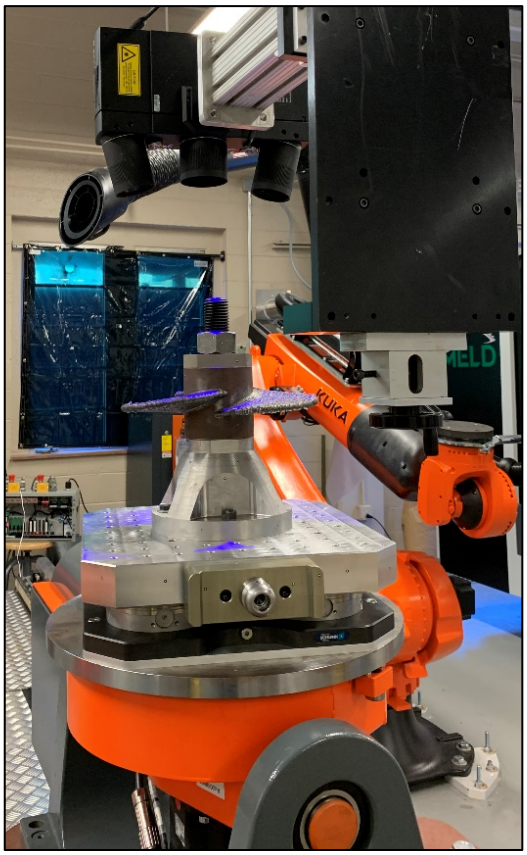


Figure 8: Post Printing Scanning

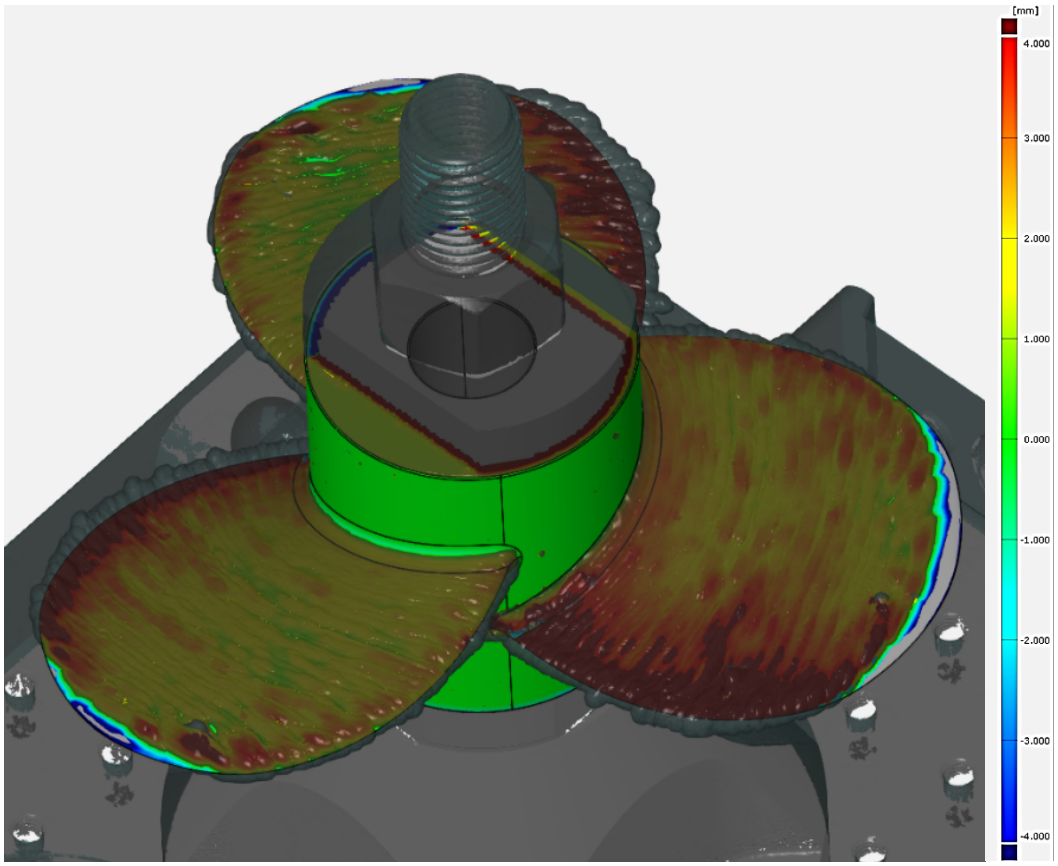


Figure 9: Post-Printing Scan Comparison for Informed Machining

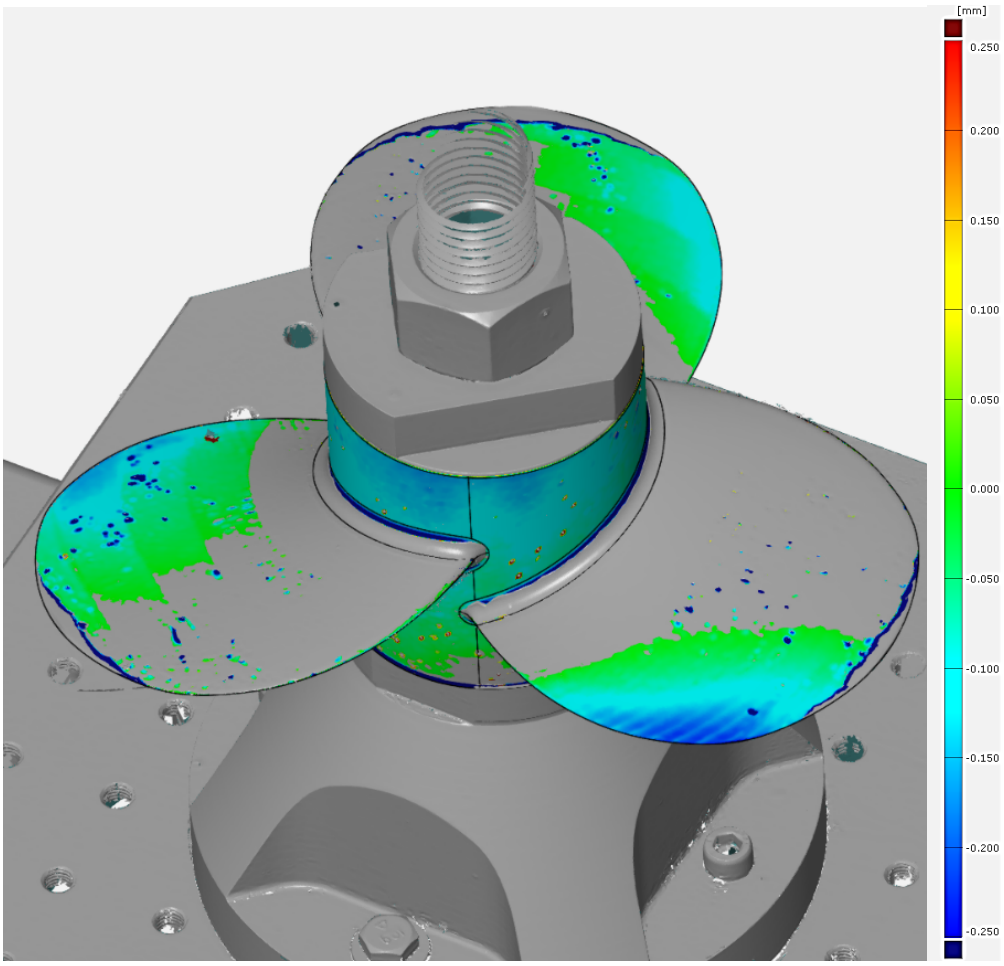


Figure 10: Post-Machining Comparison to Desired Geometry

Chapter 3

Path Planning Redundant DOF Robotic Manipulation for Wire Arc Additive Manufacturing

3.1 Welding Parameter Development for Path Planning Process

3.1.1 Bead height

In traditional MIG welding applications, two parts are joined together via molten wire adhering to each piece and creating a bond. In the additive manufacturing process, the first layer adheres to the base plate or initial substrate. This initial layer reacts differently than the remaining layers that adhere to one another. When beads are printed in succession onto one another the cross-sectional area differs greatly than if they were to adhere to a base plate. The higher the beads are printed the more the bead expands leading to loss of height. Also in traditional MIG welding applications, the temperature is kept much higher. This is due to the difference between two ambient temperature pieces being fused together in comparison to multiple layers of freshly molten wire. After printing, heat remains in each layer and must be an appropriate temperature prior to deposition of the next layer. Reduced temperature in addition to pauses between layers may be necessary to prevent overheating.

3.1.2 Wire diameter

Diameter of the wire used to weld is directly related to the amount of current and heat generated. The larger the wire, the more current is generated. With greater current comes greater heat. Additional heat causes greater concern for risk of overheating due to each layer requiring more time to cool. Longer wait times may need to be implemented between layers as a result. The risk of overheating is also augmented depending on the type of material used, some are at higher risk of overheating than others. Difference in

wire diameter also creates differences when it comes to the dexterity of the weld. Smaller wire diameters are easier to create intricate weld patterns, whereas larger wire diameters are more difficult to manipulate in a constrained manner.

3.1.3 Wait Time Between Layers

As previously mentioned, wait times may need to be implemented between layers of a print to account for heat distribution through the part. Each layer must cool to the proper interpass temperature prior to additional deposition in the next layer. This serves to reduce risk of overheating and potential damages associated. When it comes to path planning, wait functions must be implemented after each layer to allow for proper cooling. Active cooling may also be implemented to reduce the amount of wait time necessary. As the part increases in layers, wait times may need to be extended to account for heat distribution and conduction throughout the part. The more layers a part contains the more surface area heat is conducted through.

3.1.4 Contact Tip to Workpiece Distance

When creating a welding path plan, an important consideration is the distance between the contact tip of the welding torch and the workpiece the material is being deposited onto. A balance of how far the wire extends outward and the arc length of the torch is important for proper welding technique. Human welders are able to intuitively adjust and adapt this balance as they weld where robotic manipulators don’t have this sense of intuition. When this balance is disturbed, a number of errors may occur. If the torch is too close to the workpiece, the contact tip may begin to erode or may weld to the part or baseplate as seen in Figure 11. The contact tip is made of copper which has a low melting point usually mitigated by shielding gas.



Figure 11: Welded Contact Tip

If the wire extends too far from the welding torch it can break off in sections and not deposit properly. Shielding gas coverage additionally diminishes with greater distance. The equipment used in this process is a dual wire system designed to provide shielding gas to two wires depositing at the same time. Since we only use a single wire for the additive manufacturing process, the part receives better shielding gas posteriorly as it cools.

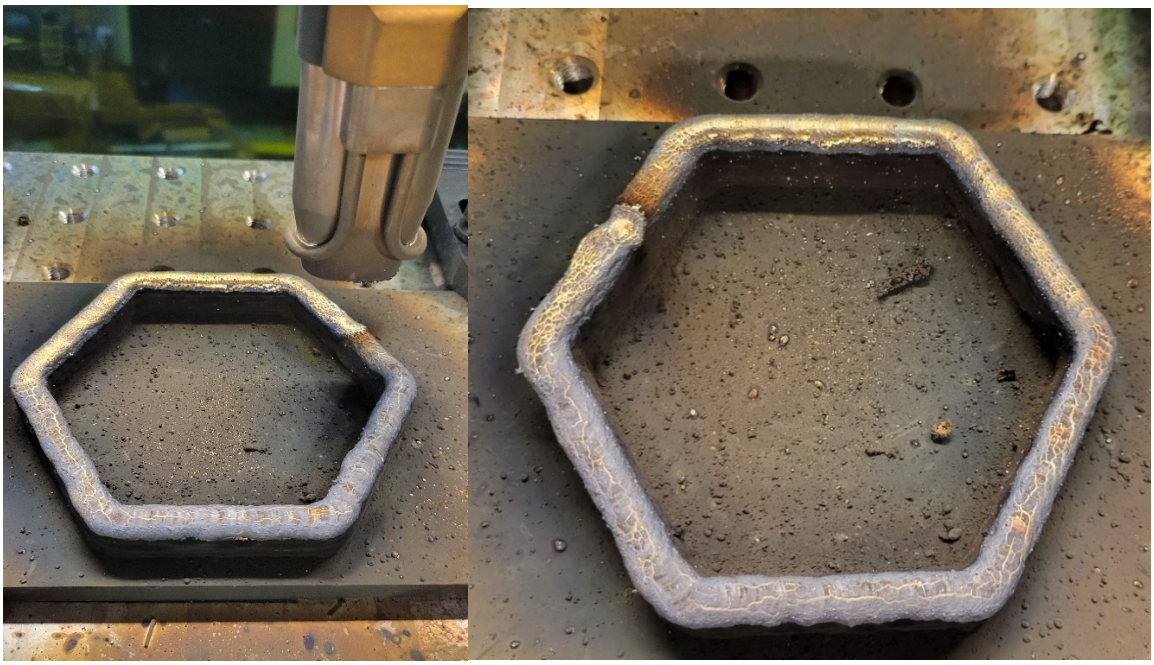


Figure 12: Shielding Gas Effects on Hexagon Build

In Figure 12 above, areas of better posterior shielding gas can be clearly seen due to the orientation of the torch along the part path. In darker areas the torch was aligned perpendicularly to the path which lessened shielding gas of material as it was deposited. For reference, the welding torch was moving in a counterclockwise path starting at the top of the image. Generally, the closer the torch is to the material being deposited results in better shielding gas. An alternative to maximize shielding gas if diminishing the distance is impractical, is to increase the shielding gas exuded. Although, this solution is constrained to an extent, for too much shielding gas will cause a vacuum to occur within the torch which pulls in excess oxygen which disturbs the weld deposited.

3.1.5 Geometry Complications

The geometry of a part may cause difficulties in printing for a number of reasons. Tight corners on a path plan cause the welding torch to have to stop and turn around between segments. When the welding torch slows down to make this turn, additional deposition of material occurs. Overlap can occur depending on how acute the angle of the turn is. This causes an upslope of the part which changes the tool to workpiece distance as the torch

welds each layer. Figure 13 below demonstrates this upslope effect of areas of additional deposition in the presence of a tight turn. Note the areas between the turns are significantly lower in height and suffered consequences of reduced shielding gas whereas the turns encountered areas of overlap and reduced tool to workpiece distance.

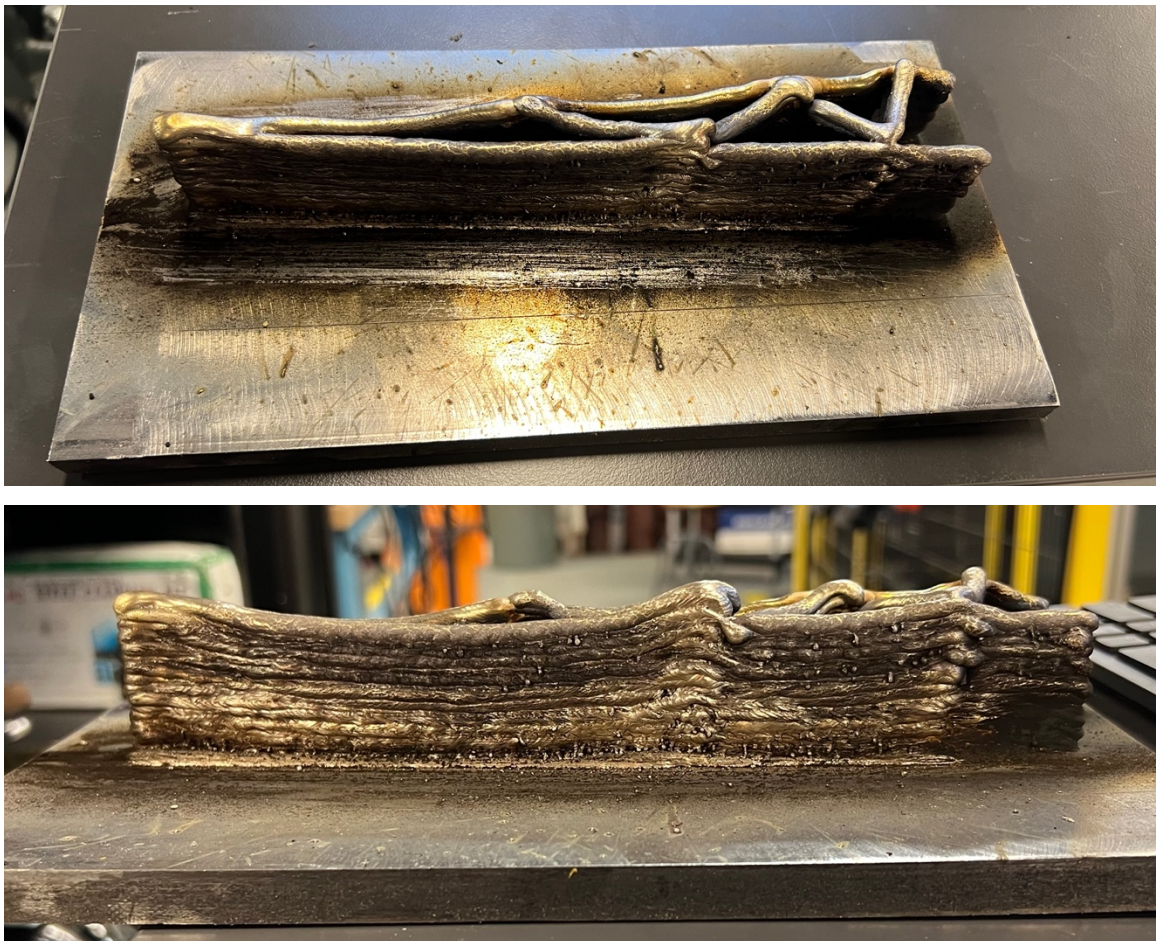


Figure 13: Warped Welds Around Turns

3.1.6 Starts and Stops

Starting a layer of a part must occur away from a corner due to the difficulty in determining the amount of material buildup that will occur. The phenomena created during a turn as previously explained, is accentuated in the instance of placing a start or stop in a corner or turn. To mitigate this, a MATLAB script is created to adjust where the

path plan of each layer begins and ends. This script visually and analytically adjusts the path plan to prevent areas of variable deposition as the result of improper placement.

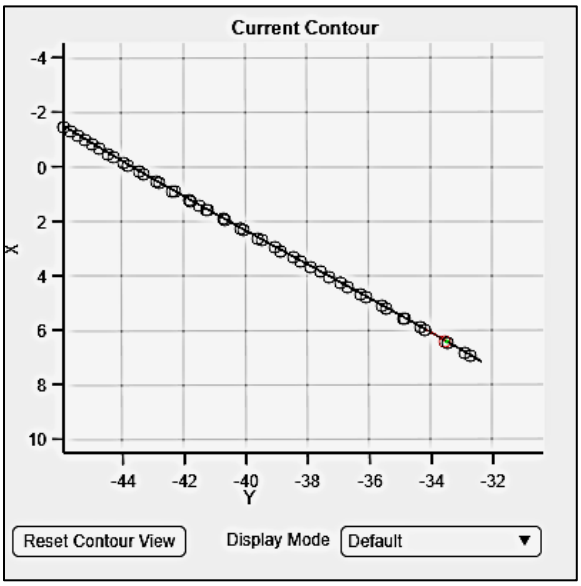


Figure 14: Graphical Depiction of Start and Stop Position

Figure 14 above demonstrates the element of the graphical user interface (GUI) used to visually analyze each contour. Each contour can be viewed and evaluated individually. This feature is necessary to determine proper placement of where the contour is to begin and end printing. The start of the build is symbolized by the green circle and the end of the build is symbolized by the red. This analysis is a crucial step to ensure proper fabrication.

3.1.7 Heat

Distortion occurs as the part cools due to contraction of the metal. The base plate experiences deformation and warps. This issue was accentuated prior to firm clamping of the base plate. Although, once the firm clamping kit is removed the plate deforms. Note the upslope on the left side of the base plate below in Figure 15.

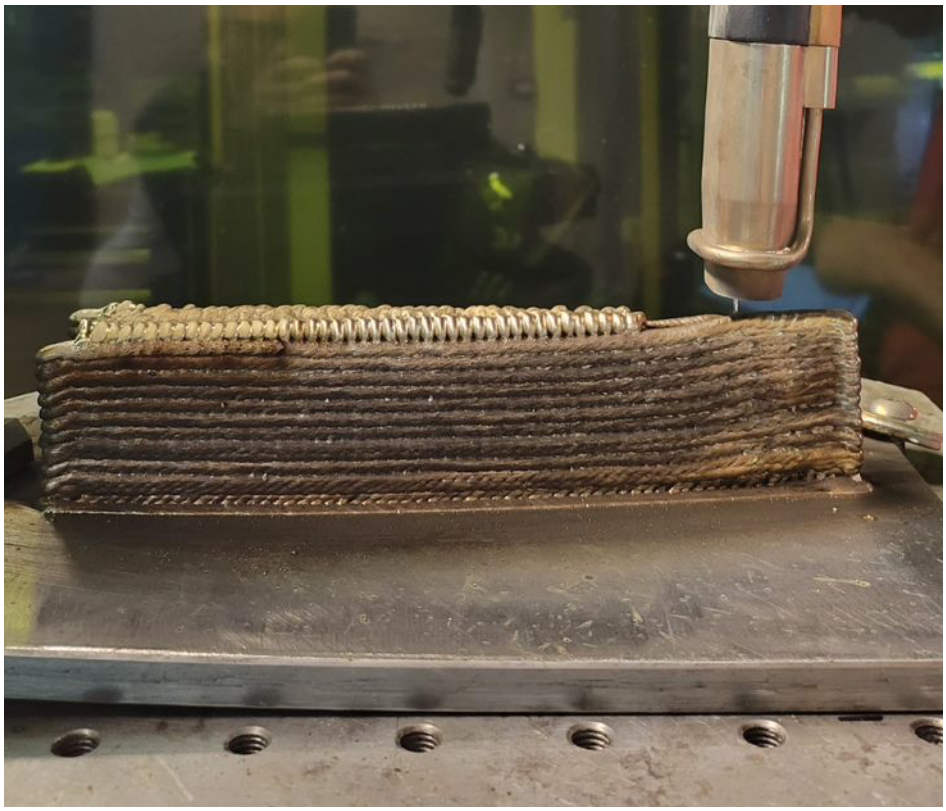


Figure 15: Base Plate Deformation

3.2 Path Planning

The process of path planning for wire arc additive manufacturing is to input a CAD model, cut it into slices to distinguish layers, export those slices through a MATLAB script to develop a path, and run a simulation of the path plan in Octopuz, a robotic simulation software.

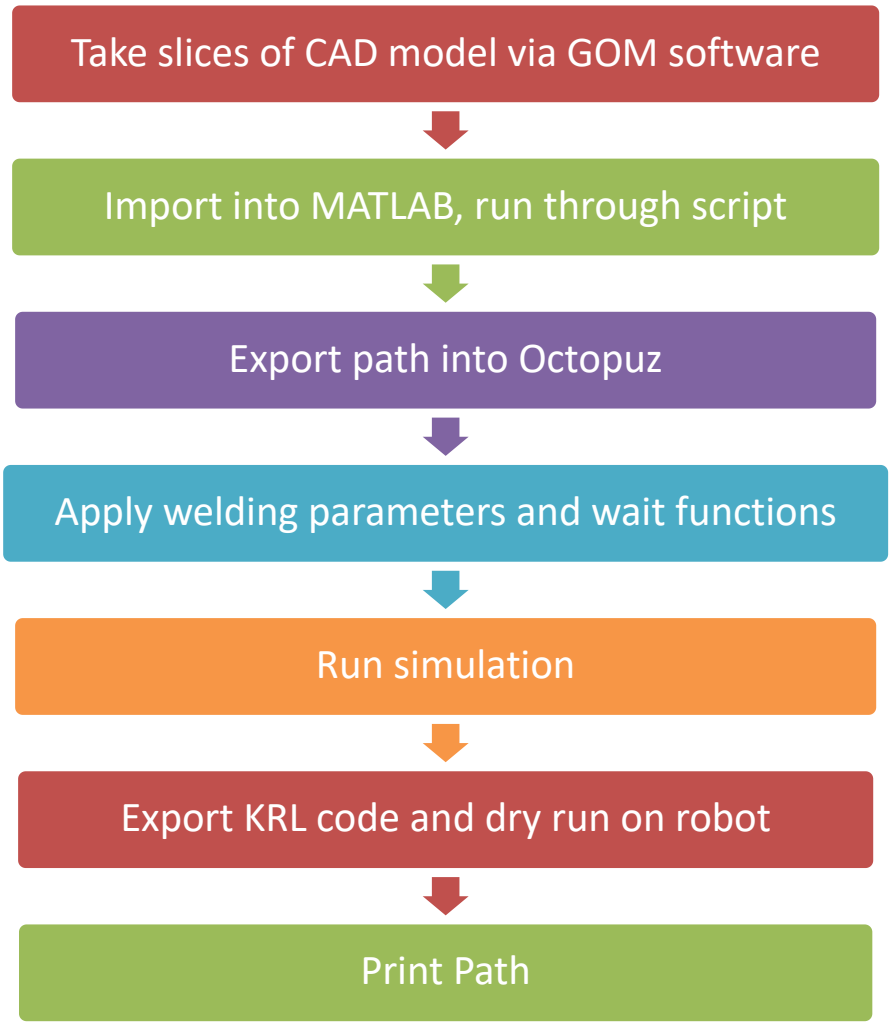


Figure 16: WAAM Path Planning Structure

3.2.1 Slicing

The first step of the path planning process is to import the CAD model of the desired geometry into GOM software. The part is then divided into "slices" that correspond to the intended layer height of the print. If the part is to be printed on a base plate, the slices are generated based off of a linear plane. If the part is to be printed on a cylindrical hub, a digital cylinder is fitted to the hub and used to radially slice the part into contours. These contours are exported as a ".ascii" file to be exported into MATLAB.

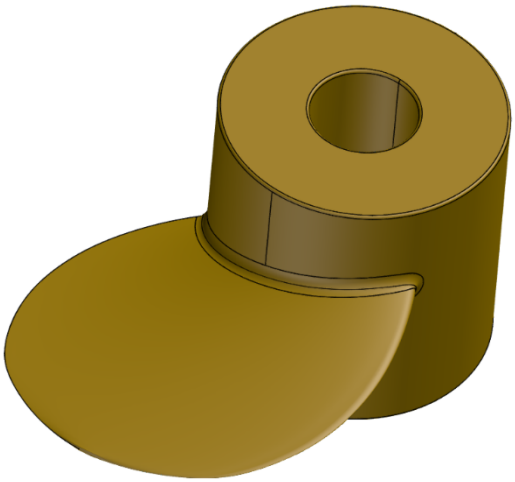


Figure 17: CAD Model Of Desired Geometry

The imported CAD model of the desired geometry is first broken into segments depending on the desired print order. In the case of Figure 17, a three-blade propeller is divided into three parts, one for each blade. By dividing the CAD into segments, each blade will be printed individually of one another instead of layer by layer of each blade in sequence.

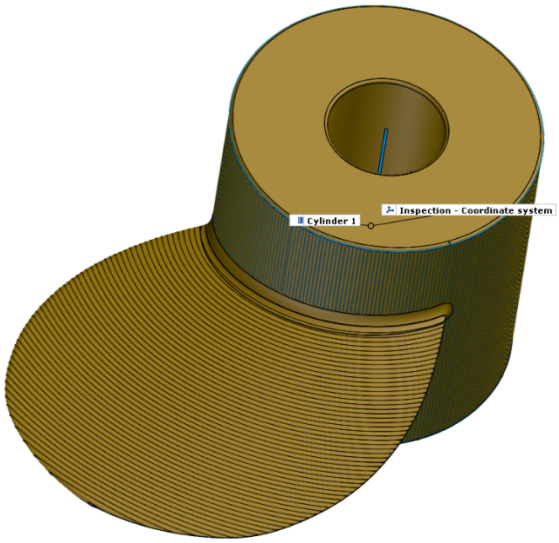


Figure 18: Cylinder Fitted, Creation of Slices

After the CAD model is broken into the desired segments, each segment is further divided into slices. This is accomplished by first fitting a baseline to where printing will

commence. In this instance, each blade is going to be printed to a central cylindrical hub. A digital cylinder is fitted to the base and used to create contour slices. The distance between the slices corresponds to the desired layer height of the weld.

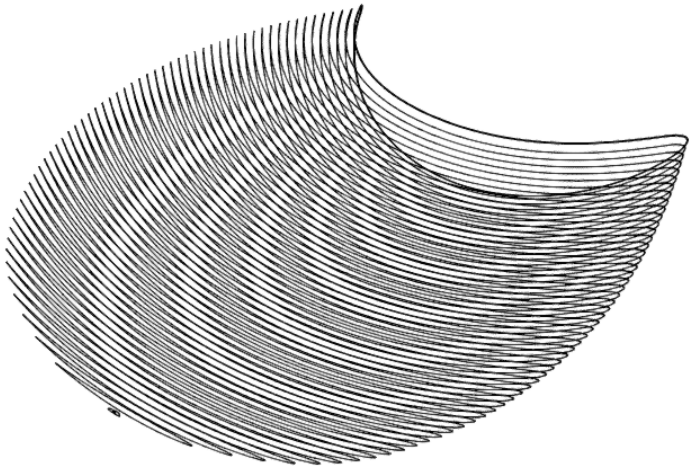


Figure 19: Slices Generated

The generated slices are exported in segments for each blade from the GOM software as ".ascii' files.

3.2.2 Importing Contours into MATLAB

The ".ascii" file is then imported into MATLAB where it is processed through a script (Figure 20, line 2) tailor made to the intended geometry. After importing, the first step of the script is to combine collinear moves (line 8) which means any consecutive points along the same path are reduced into one segment. The decimate by move length function sets the minimum move length for each contour. Direction in which the layers of the path are alternated between each layer to prevent any sloping of the part from starting continuously in one area. This also maximizes the amount of cooling time between each layer (Line 12). Segment speed is the linear speed at which the welding torch moves along each contour. This value is user defined for the specified part and material. Start points are staggered (line 16) to prevent areas of porosity and excess build up caused by starting a weld layer in the same direction for each layer. The torch angles are updated in

line 18 to keep the torch properly aligned and oriented in reference to a fixed plane of travel.

```
%% Import
p = FileTools.ImportPart('C:\Users\tquigley\Documents\GitHub\UTK-Path-Planner\PartName');

% Decimate Moves
for i = 1:length(p.segments)

    %Combine Collinear Moves
    SegmentAlgorithms.CombineCollinearMoves(p.segments{i})
    fprintf('Decimating contours to 2mm...\n')
    SegmentAlgorithms.DecimateContoursByMoveLength(p.segments{i},2);
    fprintf('Alternating contour directions...\n')
    SegmentAlgorithms.AlternateContourDirections(p.segments{i},1);
    fprintf('Updating speed...\n')
    SegmentAlgorithms.UpdateSegmentSpeed(p.segments{i},5.08);
    fprintf('Staggering start points...\n')
    SegmentAlgorithms.StaggerSegmentStartPointsByIndices(p.segments{i},10);
    fprintf('Updating torch angles...\n')
    SegmentAlgorithms.UpdateTorchAnglesUsingInterContourVectorsWithFixedTravelPlane(p.segments{i},[1,0,0])
    fprintf('Segment %i Complete!\n',i)
end


% Create Manifest
fprintf('Creating manifest...\n')
n_segments = length(p.segments);
manifest_all_simultaneous = 1:n_segments;
PartAlgorithms.ParallelizeSegments(p,manifest_all_simultaneous);

fprintf('Saving path...\n')
file_path = 'C:\Users\tquigley\Documents\GitHub\UTK-Path-Planner\PartName_manifest.path';
PathFileWriter.WritePartWithManifest(file_path,p);
```

Figure 20: MATLAB Path Script

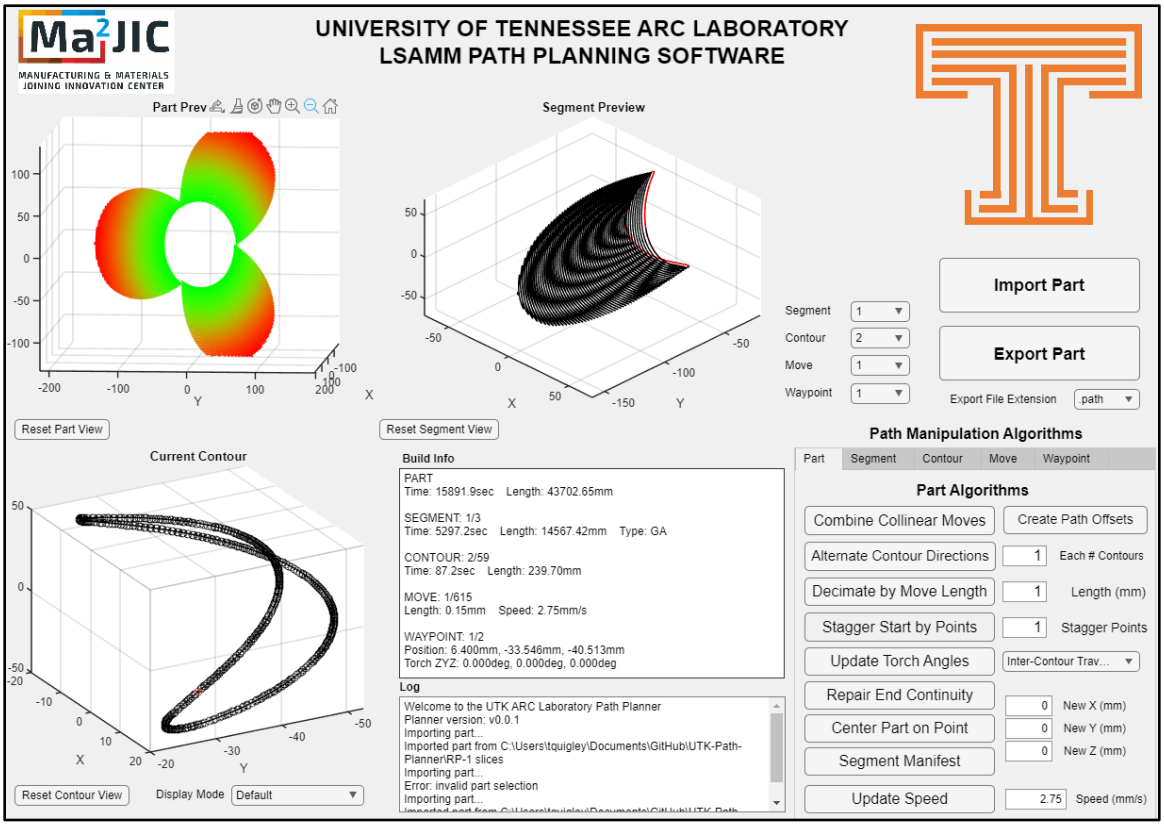


Figure 21: Graphical User Interface

After all the settings are properly maintained and adjusted, a manifest of the path is created and exported. All adjustments made in this script are also able to be seen visually in the form of the graphical user interface (Figure 21). The GUI is used to examine and verify contours are properly exhibited, starts and stops occur in proper position, and layers are in proper order. Each segment is able to be displayed individually via the GUI, and each contour of said segment is also displayed individually in the bottom right corner. Selections can be defined toward the top of the program next to the buttons for importing and exporting. Once all variables are verified and corrected, the path is exported to Octopuz for simulation.

3.2.3 Importing Path into Octopuz

The path created in the previous step is then imported into Octopuz. A replication of the hybrid manufacturing cell was previously created in Octopuz to import paths into. A new base is created to properly align the path to the part positioner. The base defines an origin and axis of where the path is in space. Once the path is aligned, wait functions are implemented after each segment of the path to allow proper cooling of the part between layers. Welding parameters are also defined in Octopuz for each layer. The first layer of the build is set to different parameters than the remaining layers to accommodate for the different cross-sectional area of the base plate in comparison to welding to a previous layer. The kinematics of the robot are manipulated as necessary to keep the welding torch gravity aligned to the part. A simulation of the path is run in its entirety to evaluate and solve any discrepancies. Once the simulation is verified, the code is exported into Kuka Robot Language (KRL) to be read by the robotic manipulator in the hybrid cell.

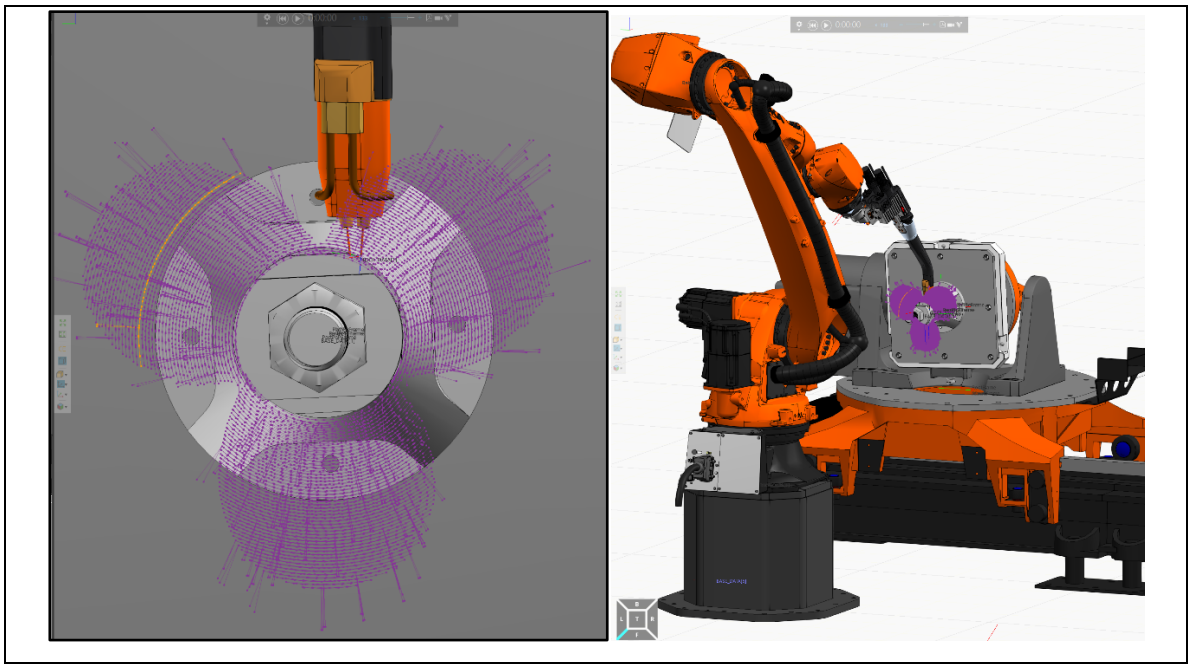


Figure 22: Path Plan Simulation

The figure above displays the path plan imported into Octopuz in purple. On the left image, the path plan generated from MATLAB is closely demonstrated with the welding torch of the robot displayed at the top of the part. The right image is the same Octopuz file, just zoomed out to reveal the configuration of the KR50 robot, KP2 part positioner, and linear track.

3.2.4 Path Plan on Robot

A new base is taught on the robot to correspond to the orientation defined in Octopuz. The KRL code generated is imported onto the robot and a dry run is administered with the torch and shielding gas off to verify the kinematics are within joint limits, workspace limits, as well as avoidance of collisions. After verification is complete, the torch and power supply are turned on and the code is set to run. The robot goes through and prints each layer as programmed. The program is closely monitored in the event that the part height gets too close to the weld torch. If the torch does come within close proximity of the part, layers may be omitted to accommodate.

A study was also conducted to ensure position accuracy of the robot when tracking the generated path plans. In this study, the path plan was administered to the robot and

various points were analyzed. When the robot reached each point, the program was paused, and the actual position of the joint axes were displayed and compared to the joint axis definitions of the program.

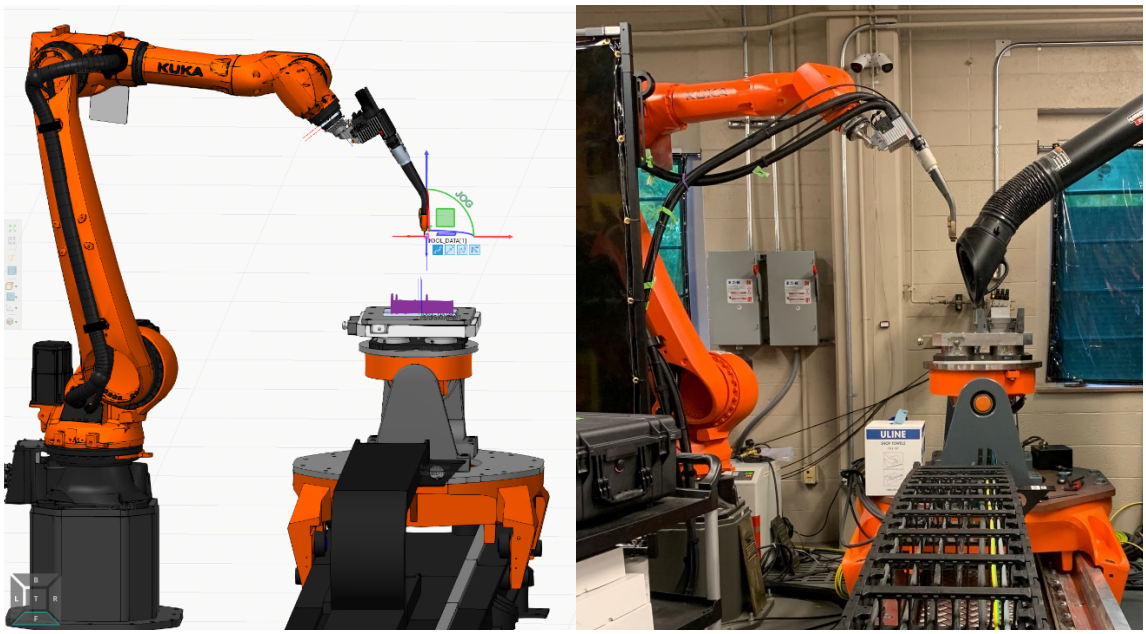


Figure 23: Joint Position Comparison Between Simulation and Actual

As seen in the table below, when running the same program to the same point, joints maintain a maximum percent error of .01% error to the intended position generated by the simulated path plan. The primary cause of error is rounding error produced by the reduction of significant figures between the simulation software and the robot.

Table 1: Comparison of Joint Axis Positions Between Simulation and Actual

	Octopuz Simulation	Robot
A1 (º)	19.398	19.40
A2 (º)	-102.112	-102.11
A3 (º)	105.964	105.96
A4 (º)	-14.875	-14.88
A5 (º)	49.523	49.52
A6 (º)	25.716	25.72
E1 (mm)	-3000.000	-3000.00
E2 (mm)	0.000	0.00
E3 (mm)	-55.000	-55.00

3.2.5 Coupling of the Part Positioner

Traditional configurations of KUKA robotic consist of mounting a 6 DOF robotic manipulator atop of a linear track (Figure 24) or secured in a fixed position to the floor (Figure 25). Mounting the part positioner to the linear track as configured in the hybrid manufacturing cell, introduced a new unique arrangement of the robotic units that KUKA had not yet explored. This created challenges in coupling the part positioner to the robot for a traditional part positioner remains in a fixed position in relation to the root of the 6 DOF robotic manipulator.

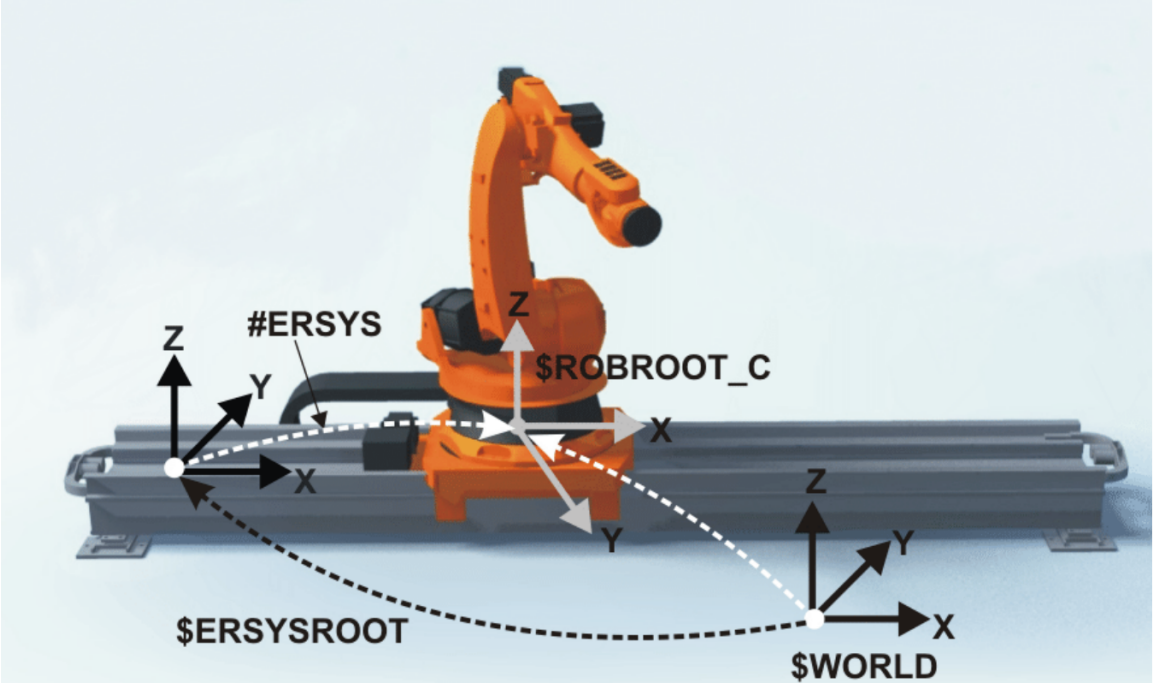


Figure 24: Kinematic Chain of Robot Mounted to Linear Track (KUKA Robotics, 2017)

By mounting the part positioner to the linear track this traditional coupling process could not be performed for the origin that would be taught on the part positioner would translate along the linear track as the part positioner translates. Figure 25 below demonstrates the relationship between the 6 DOF robot and the robotic manipulator. Note the root of the robot and the root of the part positioner are both taught in relation to a fixed origin in the world frame. However, in the setup of the hybrid cell, if the linear track were to move the part positioner, the new position of the root of the part positioner would not be known in relation to the world frame.

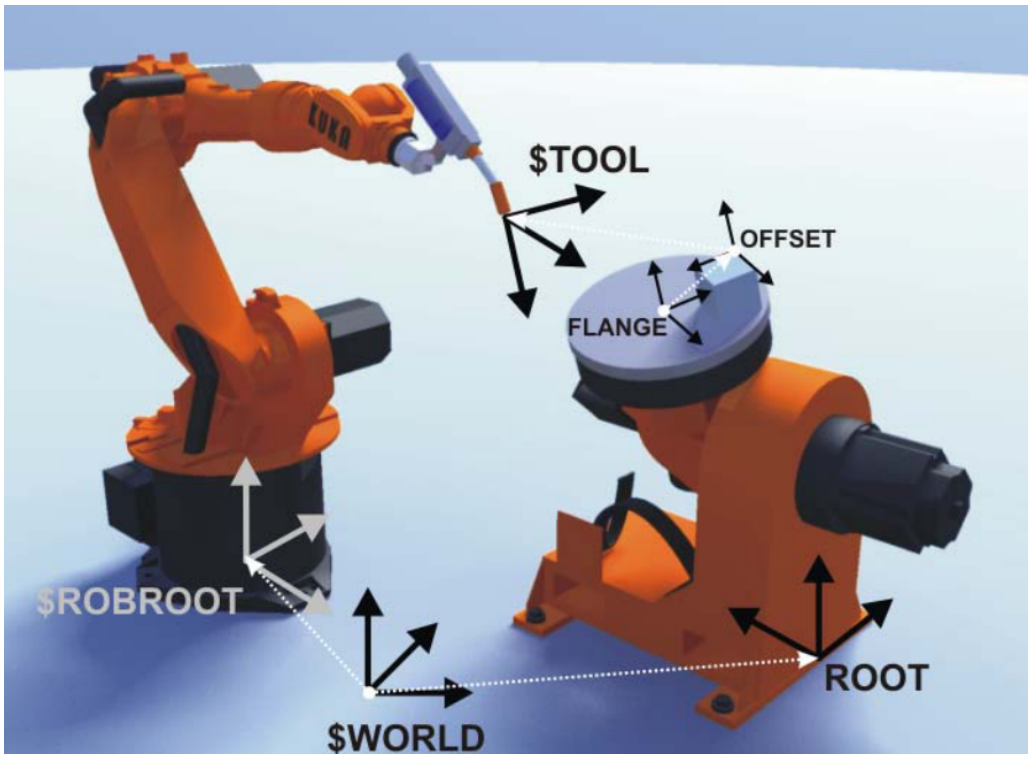


Figure 25: Robot and Part Positioner Kinematic Chain (KUKA Robotics, 2017)

When first attempting to couple the part positioner to the robotic manipulator, an offset in alignment occurred between the part positioner and flange of the robot (Figure 26). The cause of this offset was later attributed to the loss of communication between the world coordinate frame origin and the root of the part positioner due to translation along the linear track. At the time, KUKA software did not support this configuration.

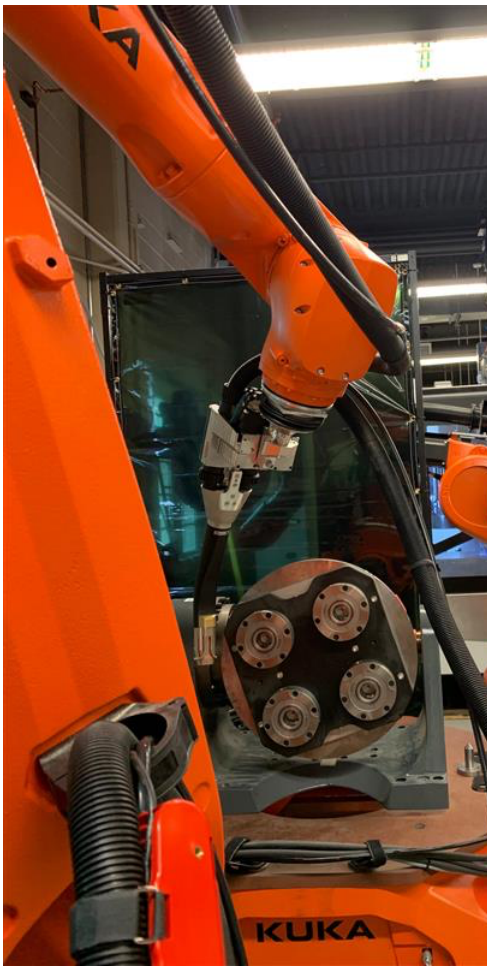


Figure 26: Offset between KR50 and Part Positioner

As a result, the KPL3 system was developed by KUKA to accommodate this new system structure. The KPL3 treats the part positioner and linear track as one Denavit-Hartenberg system in relation to the K50 (Figure 27).

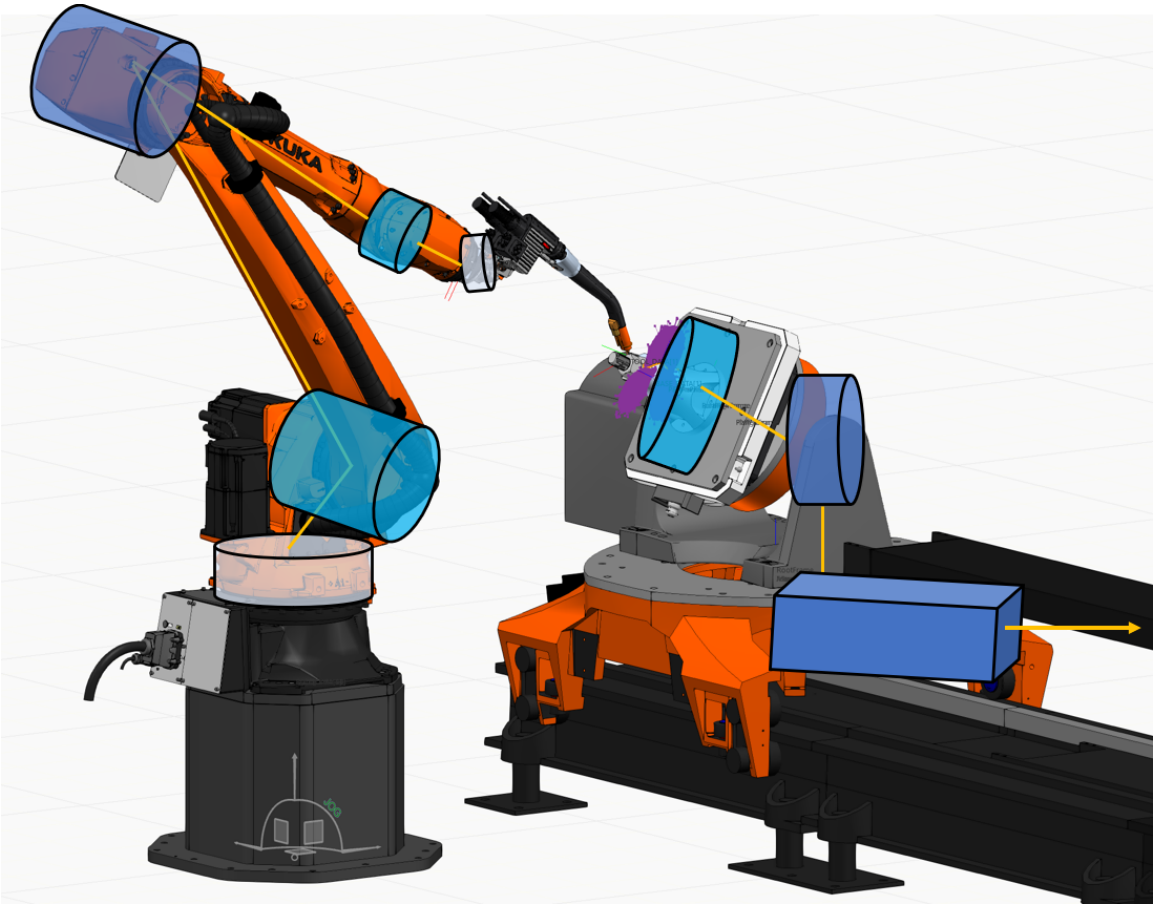


Figure 27: Denavit-Hartenberg System Containing KR50 and KPL3

Chapter 4

Mounting of Scanner to Robot

4.1 Hardware Design

The mounting fixture created to secure the 3D scanner to the KR250 is comprised of Al6061-T6 aluminum for ease of manufacturing as well as cosmetic appeal. This material is easy to machine, readily accessible, and easily refined to a smooth finish. The mount is step machined about the Foba BALSA mounting bracket (Figure 28) used to attach the scanner to this fixture. This is necessary for the locking feature (red handle seen below) to successfully secure the camera into place in any orientation. Four M5 threads on the topside of the bracket permit direction versatility in which the camera can be mounted. An additional 3/8 threaded incision was made below the mounting bracket for optional additional security of the camera. Due to the camera's weight being only 8 pounds, this was later deemed unnecessary.

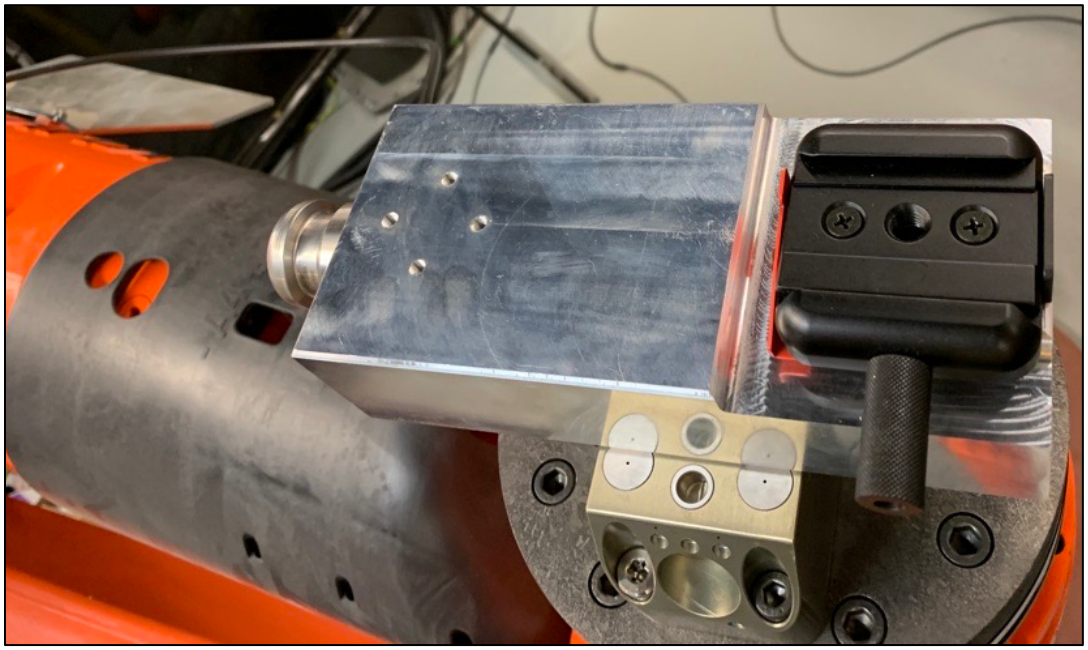


Figure 28: GOM Scanner Mounting Bracket

A Schunk pneumatic gripper applies 1100 pounds of omnidirectional clamping force to secure the mount to the gripper of the robot. These particular mounts were chosen for their compliance and lack of play once secured. Because the mounts clamping force is omnidirectional, careful attention to the orientation of the camera must be taken into account. Implementing two mounts allow for the camera to be affixed either perpendicularly (Figure 29) or in line with the end effector (Figure 30). In the developmental stage of mounting the scanner, this allowed the mount to act as a test bed for each orientation to determine the optimal kinematic configuration of the scanner.

4.2 Straight vs. 90 degree Configuration

4.2.1 Kinematics

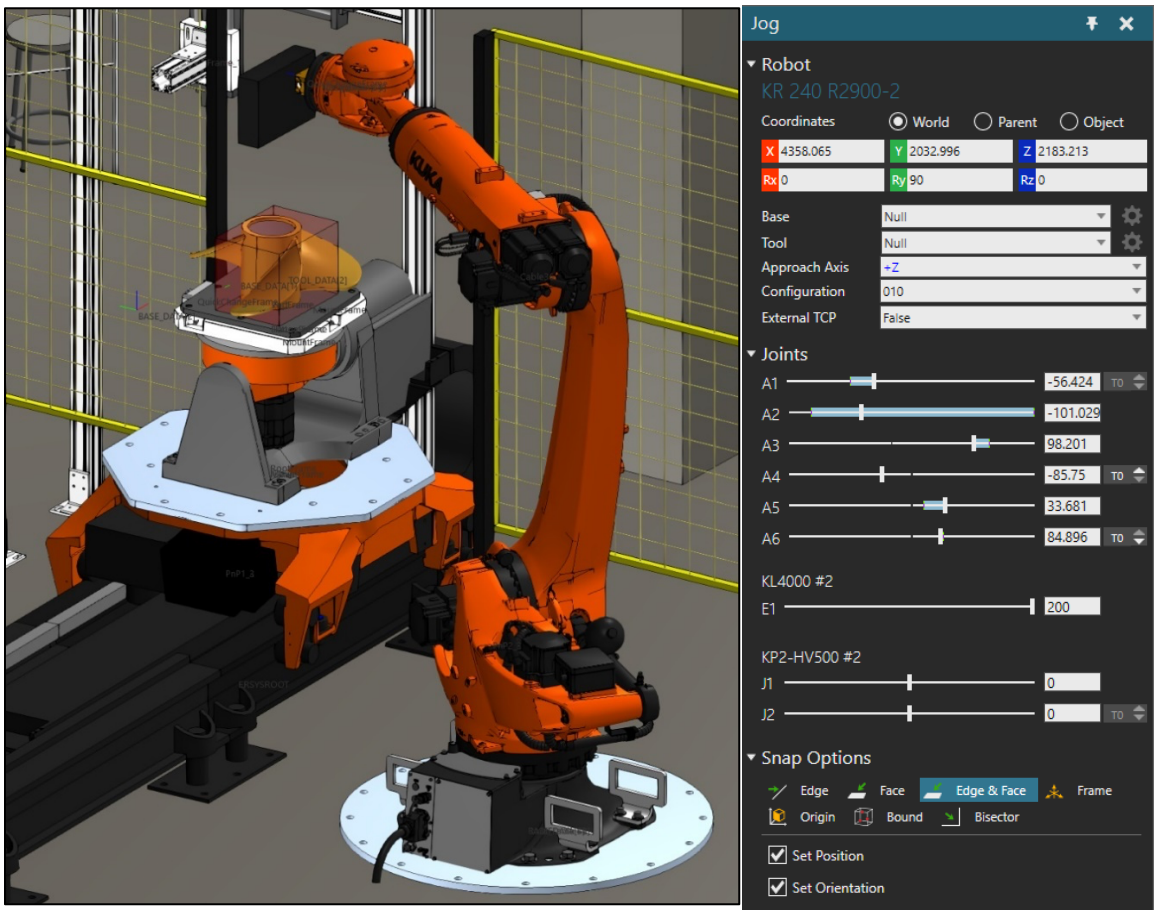


Figure 29: Scanner Mounted in 90 Degree Configuration

As seen in Figure 29 above, all kinematics of the joints remain within the joint axis limits. Limits of each joint are depicted on the right-hand side of the figure. Each end of the slider represents a limit, meaning the closer the slider is to the middle the further it is away from both limits of the joint. Limits for all 6 degrees of freedom are depicted denoted as A1 through A6. Apart from joint axis 2 (depicted as A2), most joints hardly require movement when performing a scanning simulation. The same simulation path plan was used for both the straight and 90-degree configuration of the scanner.

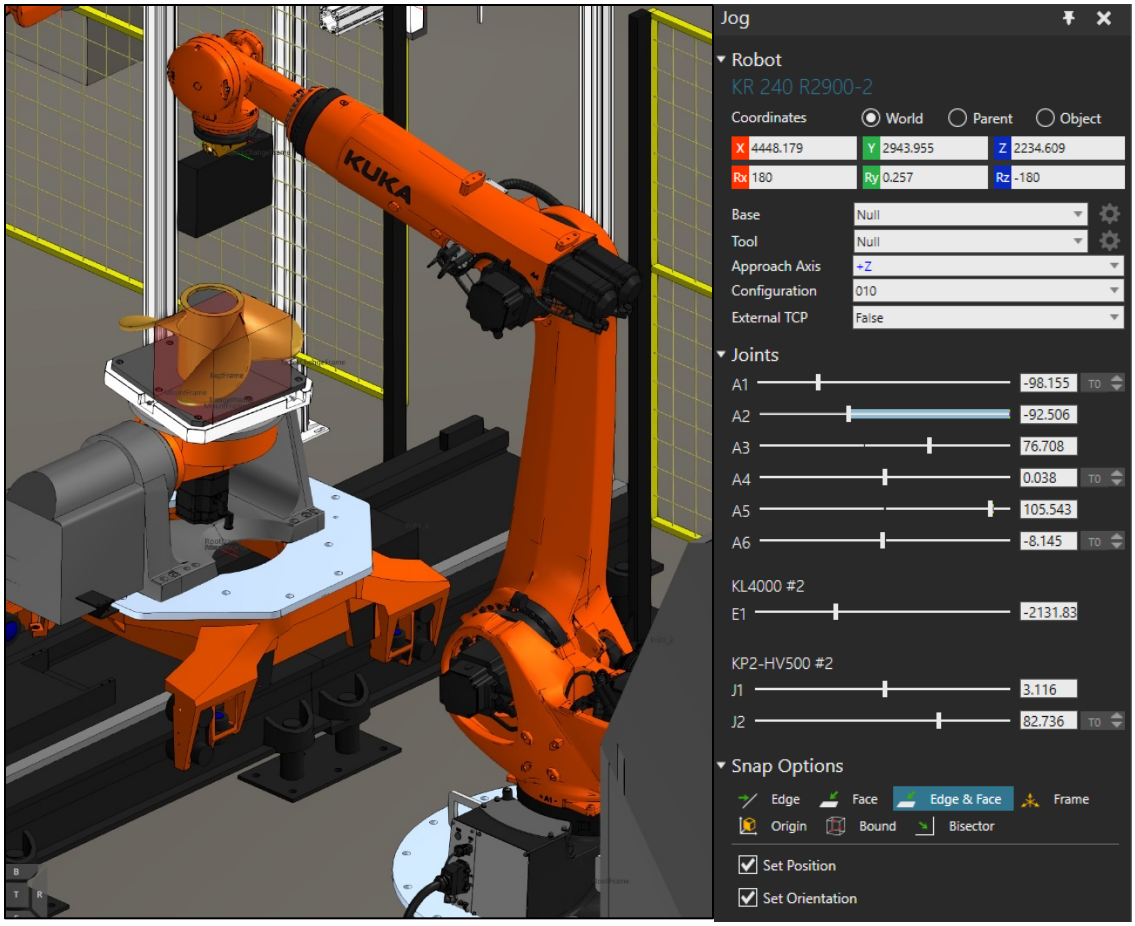


Figure 30: Scanner Mounted In Line With End Effector

When the same simulation is performed using the scanner in a zero-degree configuration, both joint axis 2 (A2) and 5 (A5) come within close contact with their joint axis limits. With regard to these considerations, the 90-degree mounting configuration of the scanner was selected for the final design.

4.2.2 Collision Avoidance

When the scanner is mounted in the straight configuration in relation to the end effector of the robot, visibility of the part is dramatically reduced. Maintaining visibility of the part requires more kinematically complex movements, as well as increases risk of collision of the part. Maneuverability and respective field of view of the camera become a challenge when confined to the limited workspace of the hybrid manufacturing cell. As seen in Figure 31 below, the camera collides with the part when performing the same

scanning path plan the 90-degree configuration was able to run successfully. Also note, the robot is at a joint axis limit for A2 meaning, it cannot collapse any further. Therefore, the path plan would need to be adjusted for primarily topside views, limiting visibility of more complex geometries.

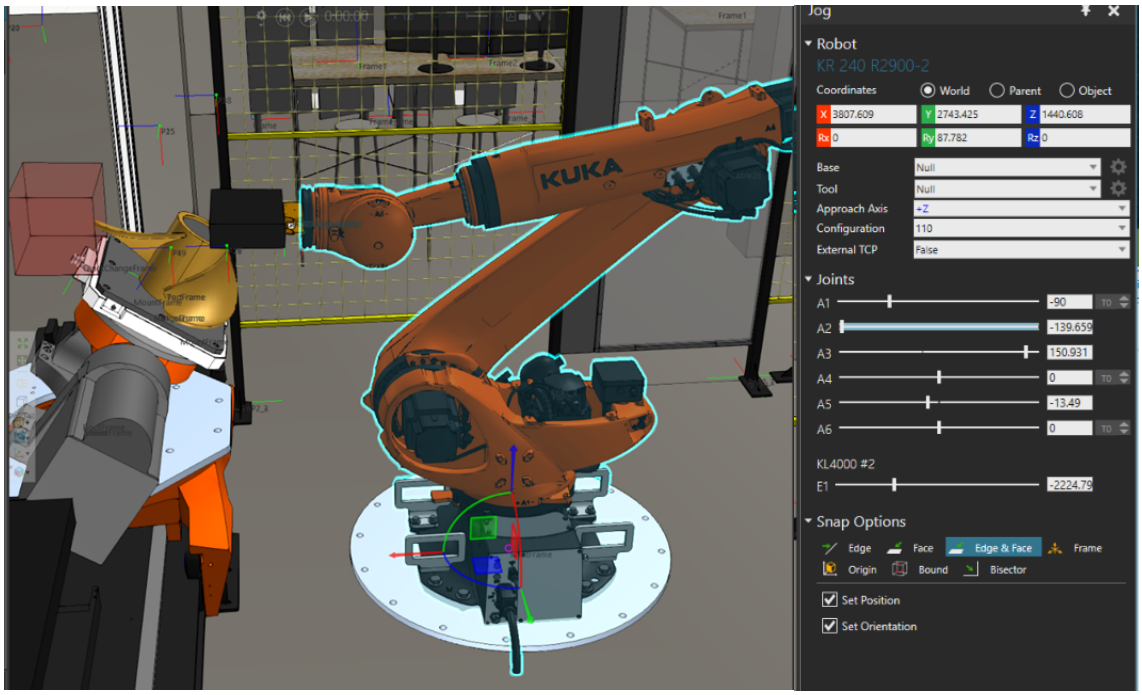


Figure 31: Collision in Straight Scanner Configuration

4.3 GOM Software

4.3.1 Sufficient Reference Points

An important factor to consider when using the robotic manipulator to scan a geometry is remaining within range of sufficient reference points. Fiducials are placed along the baseplate that a part is to be printed onto and are used by the camera to determine its position in space and in relation to the part. The camera must remain within view of at least 3 reference points to administer a successful scan. A preview displaying which fiducials are visible, and those that are unusable to the scanner and whether the unusable reference points are labeled are too close or too far on the display.

4.3.2 Field of View

The field of view of the scanner is visible as a segmented box displayed on the GOM Inspect software while scanning is conducted. A red plane dictates the optimal plane for the surface to be aligned to best acquire accurate data. Fiducials appear as green reference points once within view of the scanner.

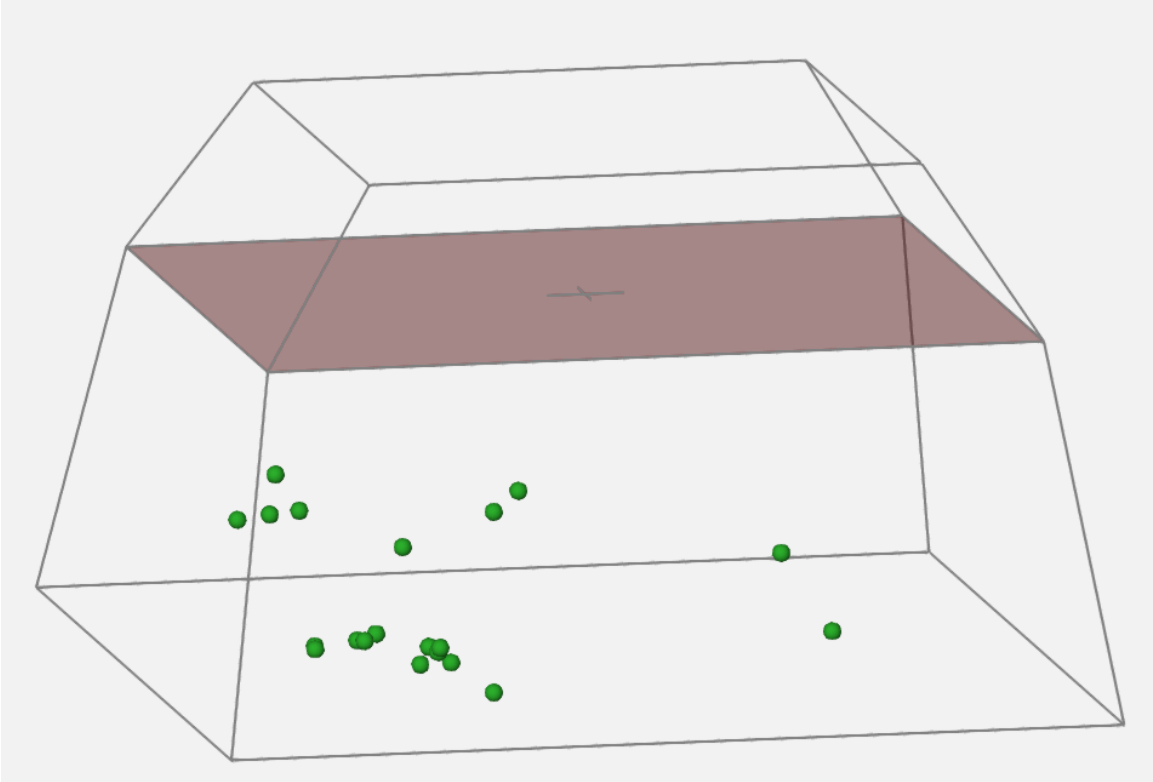


Figure 32: Scan Volume

4.3.3 Scan Result Using KR250

The KR250 was used to scan a tall walled hexagon geometry by hand jogging the scanner into place via the smart pad for each scan acquisition as seen below. Once in position, the scanner was actuated and given adequate time to determine its position and administer a scan.



Figure 33: Scanning via R250

Below demonstrates the result of 47 scans using the robot to orient about the part. Data collection using the scanner mounted to the robot resulted in great success with minimal areas of data dropout, large areas of data acquisition within a single scan, and minimal time required to translate from position to position. Figure 35 shows each position the robot was moved to in relation to the part to acquire all 47 scans. In its totality, this scan process was performed in under one hour.

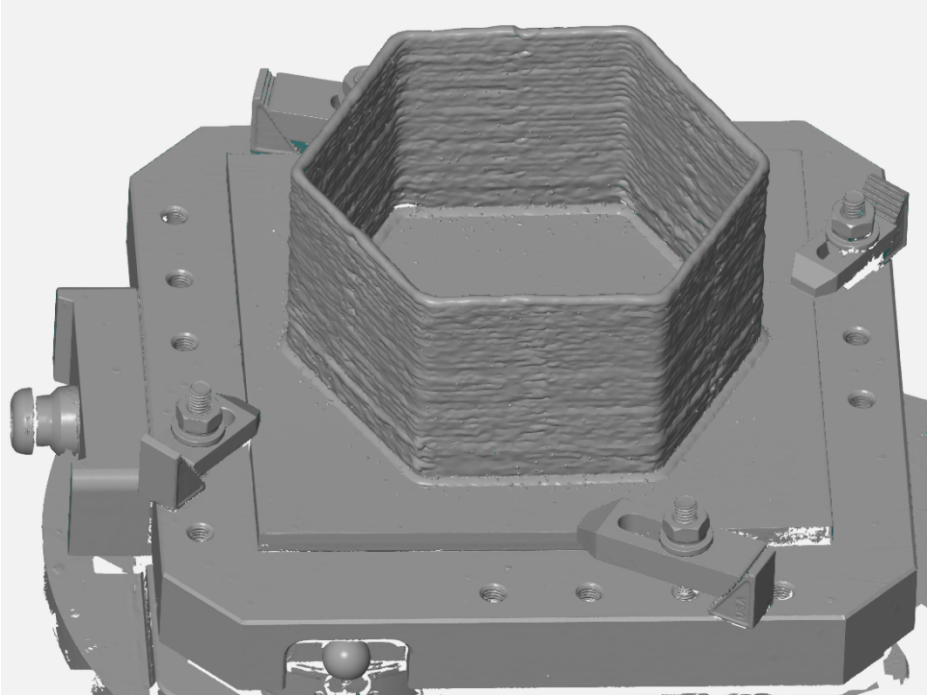


Figure 34: Scan Results of Hexagon Using KR250



Figure 35: Hexagon Scan Image Map Using KR250

Chapter 5

Path Planning for Scanning

5.1 Motivation

Metrology is an integral necessity for informed machining to occur. When first incorporating metrology into the hybrid cell, the process was arduous, time consuming, and scans were of minimal quality. Manual scanning from a static configuration was more time consuming than printing, dramatically affecting lead time to produce a part as discussed in 5.2 below. Data dropout was prominent in areas of porosity from the printing process and posterior portions of the geometry. Hundreds of scans were necessary to generate an image of sufficient quality for informed machining.

5.2 Static Configuration Scanning

5.2.1 Static Configuration Camera Straight Down

Prior to mounting the ATOS Q to the KR250 robotic manipulator, scanning was performed manually via manipulation of the part positioner and scanner repositioning via translation. The scanner was positioned in a static mount that was strictly able to translate in the x and z axes via handwheels as seen in Figure 37 below. Though the scanner was able to translate about these two axes, the physical mounting and orientation of the camera in relation to the fixture is fixed, meaning the camera is unable to point in any direction other than what it is initially mounted in. Figure 36 below demonstrates the fixture as a whole (left) as well as the contact point of the camera in relation to the fixture (right). The physical mounting point of the camera is unable to move, hence the term static. However, the fixture as a whole is able to translate vertically and laterally. Design of this configuration was motivated by the intent to later automate the scanner placement by replacing the handwheels with servo motors to translate the scanner more efficiently.

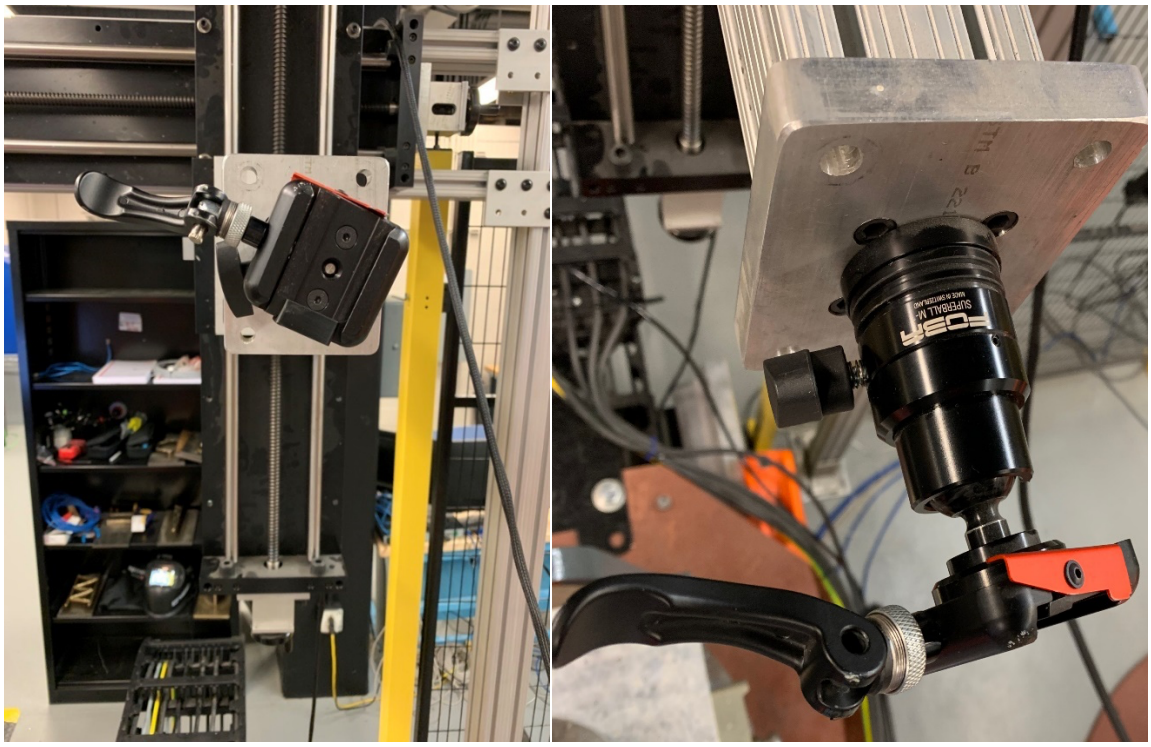


Figure 36: Static Configuration Mount for Scanner

The smart pad was used to tilt and rotate the part positioner respective to the scanner placement between each scan for ideal imaging. The part positioner is mounted on top of a linear track which makes it feasible to easily translate the part from printing to directly beneath the scanner.

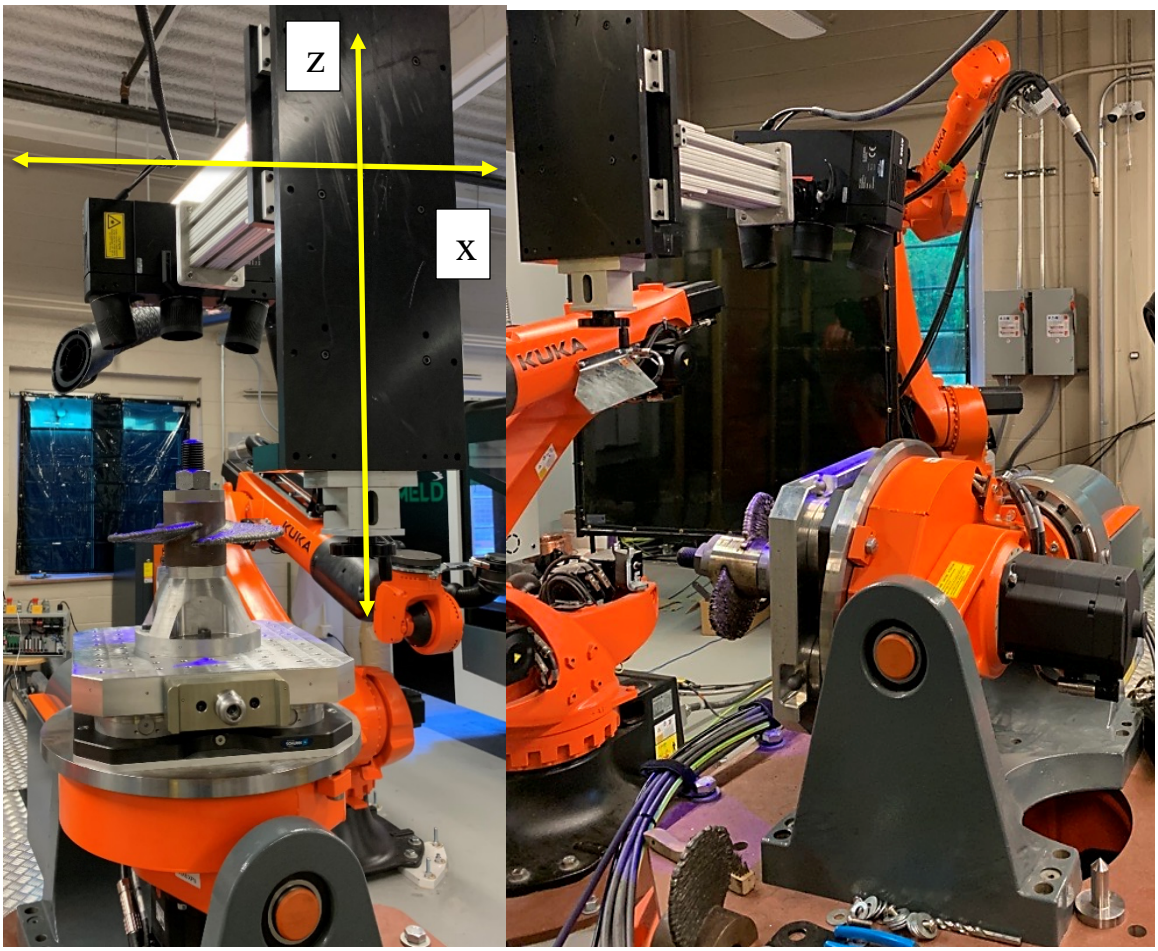


Figure 37: Static Configuration of GOM ATOS Q Scanner

As previously mentioned, this method of scanning experiences large areas of data dropout predominantly caused by obscuration. Areas of porosity that occurred in the printing process engendered posterior shadowing where the blue light was unable to reach and therefore was unable to be received and processed by the cameras. In more complex geometries, a portion of the part overshadows another leading to data dropout on account of lack of visibility. Obscuration also occurs on account of the part positioner overshadowing the part at higher tilt angles.

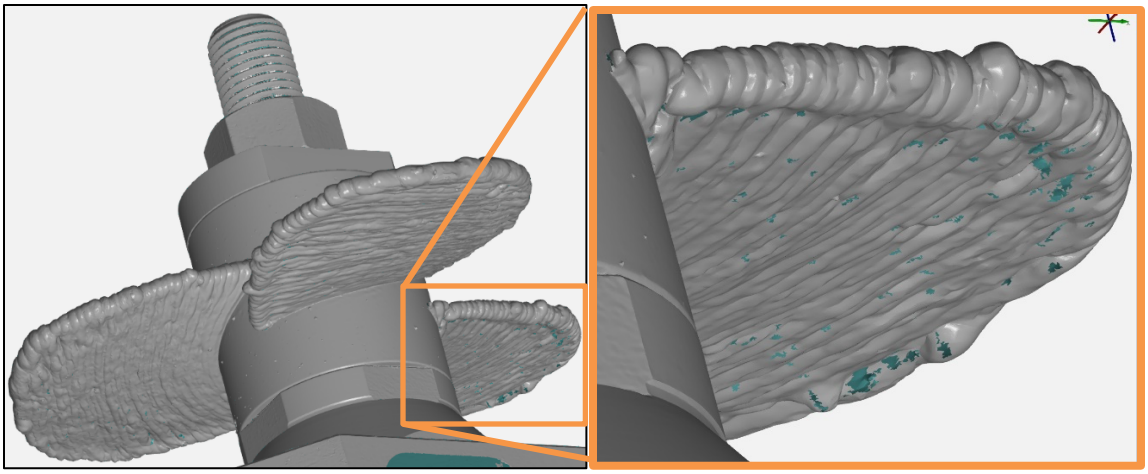


Figure 38: Result of Scanning in Static Configuration

Figure 38 above is a culmination of 535 scans, areas in blue indicate areas of data dropout. This scan required 6 hours to perform manually given the procedure described above. This includes the time required to hand crank the scanner into each position, rotate and tilt the part positioner into position, and administer the scan. Even if this process was automated using the original intention of servo motors in lieu of the hand wheels, assuming 30 seconds per scan would still put the scanning process at a time requirement of nearly 4.5 hours. To gain perspective, printing takes approximately 3-4 hours and machining only takes about an hour.

5.2.2 Implementing 25-Degree Mounting Angle

Through experimentation it was determined that mounting the scanner at a 25-degree angle in relation to the static mount produced better images and reduced the number of scans required to produce an image of sufficient quality for informed machining. Mounting the scanner at this angle largely reduced overshadowing of the part positioner and allowed for easier visibility of the posterior areas of the part. A depiction of the configuration is below in Figure 39.

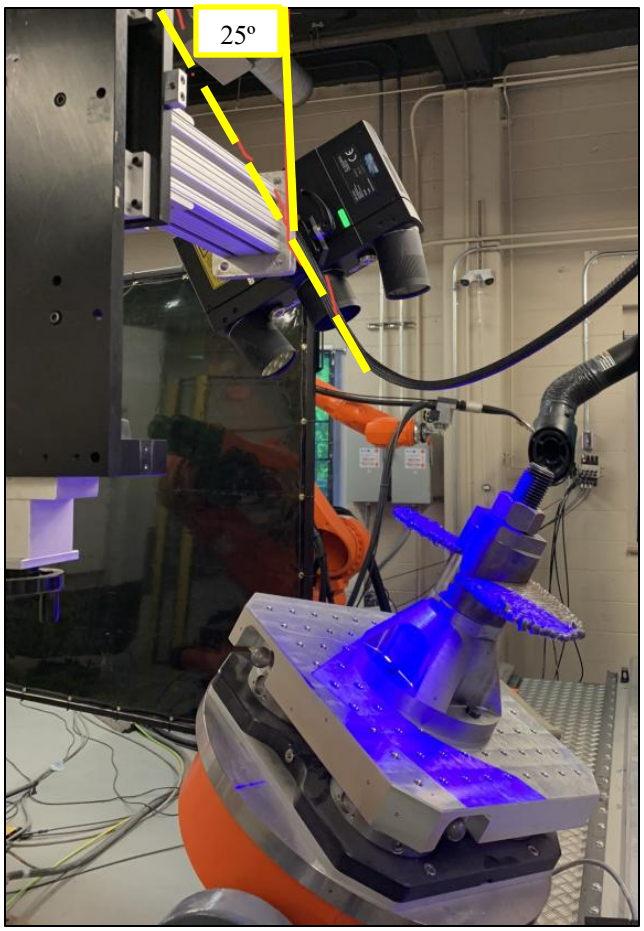


Figure 39: 25-degree Scanner Mounting Angle

When using the scanner at this angle, only 189 scans were required to construct a sufficient image for machining. In an automated process, this adjustment would reduce scan lead time by 65%, leading to a reduced scan time of approximately 1.5 hours. This slight adjustment reduces scan time to less than half of the time necessary to print. Figure 40 below shows the scan results of this configuration. Though areas of data dropout are prominent along the edges of the blade where porosity had occurred, enough data was collected to be sufficient for informed machining.

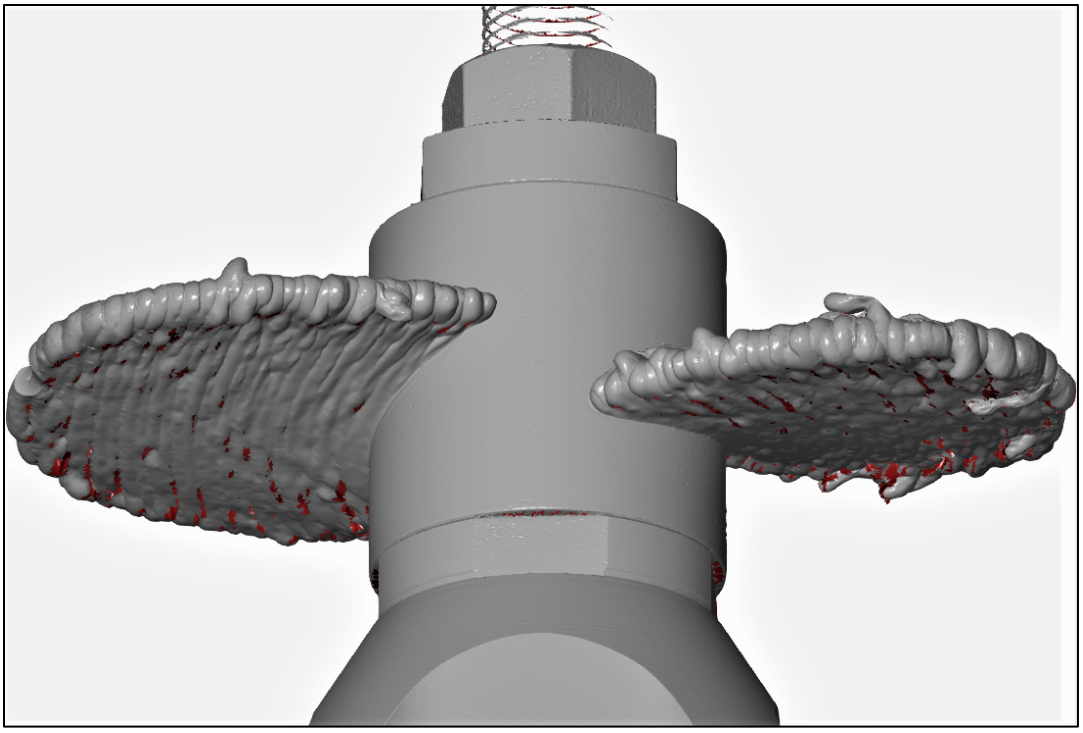


Figure 40: Scan Results of 25-Degree Configuration

5.3 Scanning View Constraint Study

Data analysis of the field of view of the scanner was conducted via a gage ball study. In this study, Figure 41 represents a polygonized mesh comprised of 5 scans. A single scan was extracted from this data set and compared to a gage ball of known diameter to determine the amount and quality of data acquired in a single scan. A surface inspection was performed via GOM Inspect Pro software; this directly compares the scan surface to an imported CAD model of the geometry. A section through the center of the sphere was cut and equidistant reference points were placed along the section. The coordinates of these reference points were exported into an excel file for further analysis.

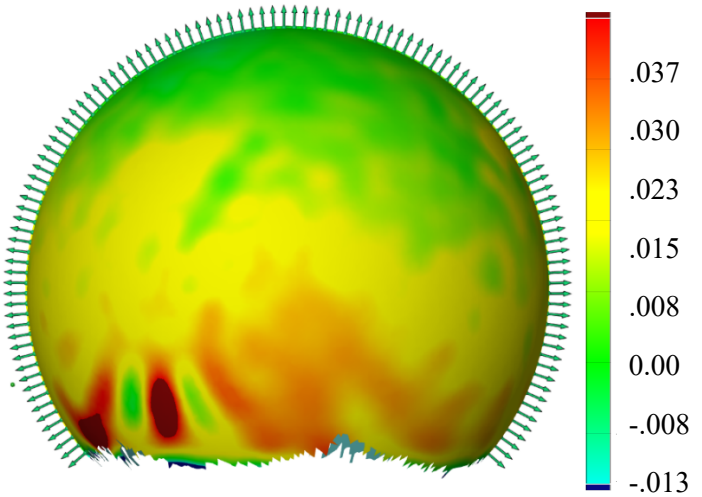


Figure 41: Gage Ball Study

As expected, the top surface of the geometry scans with the utmost accuracy, and data reliability decreases as the surface curves away from the scanner. The intent of this date analysis is to determine where data dropout is most likely to occur and articulate the camera respectively to optimize the scanning process. The first procedure step performed determined the error of a reference point of the scan in relation to its intended position dictated by the CAD model. The error between the actual reference point position in comparison with where it should be dictated by the CAD model is compared to the angle in relation to the scanner. The data analysis approach of defining angle deviation is inspired by the journal article “Development and Verification of a Novel Robot-Integrated Fringe Projection 3D Scanning System for Large-Scale Metrology (Du, Chen, Xi, Yu, & Zhao, 2017)” which used angle determination in relation to error to determine ideal scanning configuration of large-scale parts. In this paper a robotic manipulator was guided by a laser to orient the scanner into the desired configurations whereas the intent here is to implement angle constraints into the path planning process.

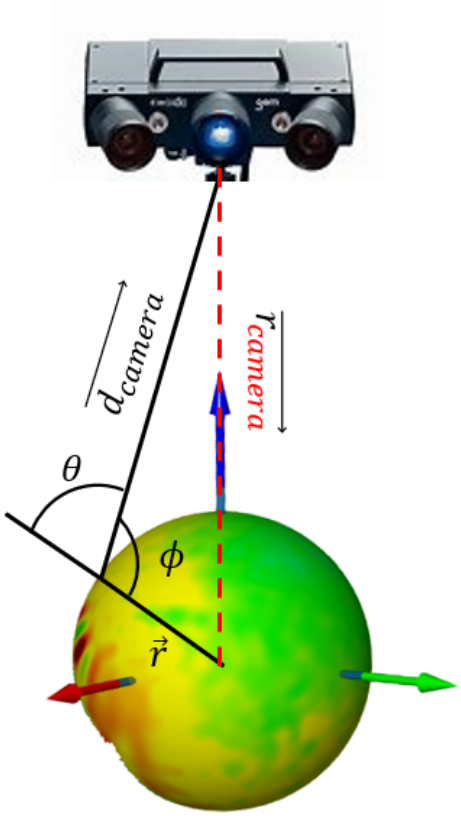


Figure 42: Schematic Description of Data Analysis Conducted

Figure 42 above depicts the analytical relationship used to determine the angle phi relative from each reference point to the scanner. To perform this analysis, vectors were derived from the arrangement depicted in Figure 42 using the following equations:

$$\vec{d}_{camera} = \sqrt{x_{camera}^2 + y_{camera}^2 + z_{camera}^2}$$

$$\vec{r} = \sqrt{x^2 + y^2 + z^2}$$

$$\phi = 180 - \frac{\vec{r} \cdot \vec{d}_{camera}}{\|\vec{r}\| \, \|\vec{d}_{camera}\|}$$

Error was quantified as the difference in millimeters between the scan acquisition and the surface of the CAD model of the gage ball.

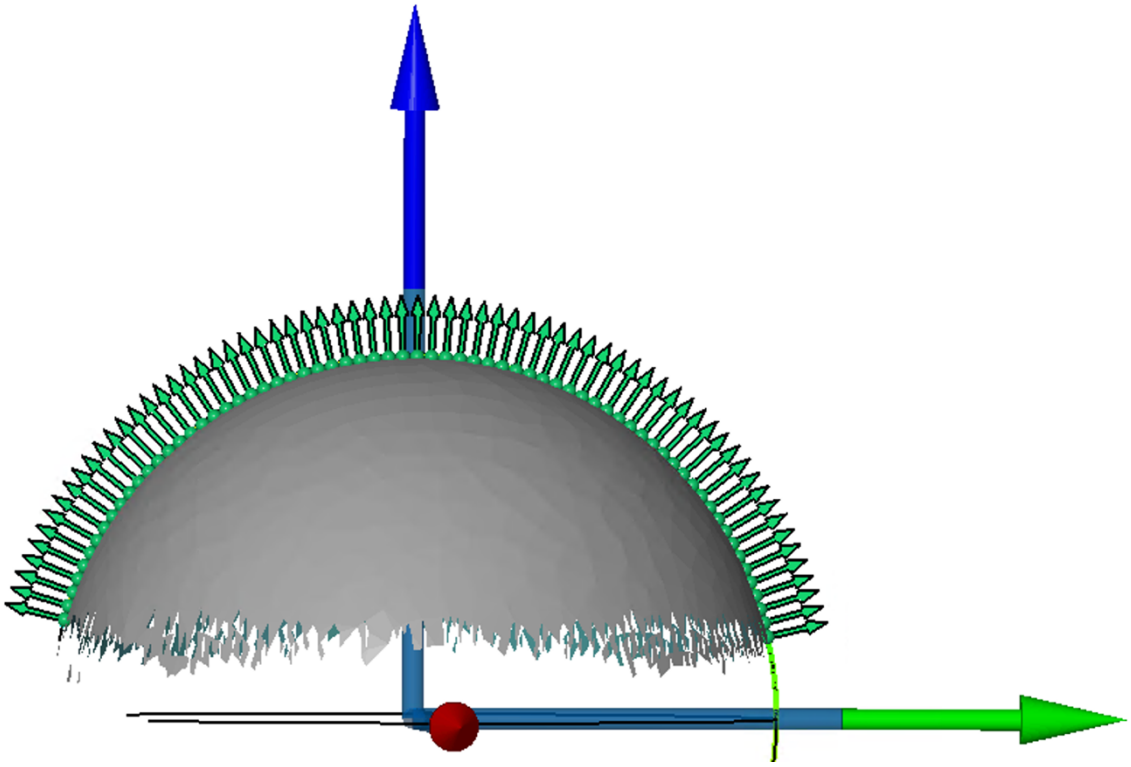


Figure 43: Single Scan Data Set

Figure 43 above displays the amount of data able to be collected in a single scan. The equations mentioned and depicted previously were used to determine the exact angle limit to where data can no longer be collected and the ideal angle in which a scan should be administered for optimum data collection. A series of reference points were evenly distributed along a section of the scan and compared to the CAD model of the known geometry. This data is represented in graphical form in below.

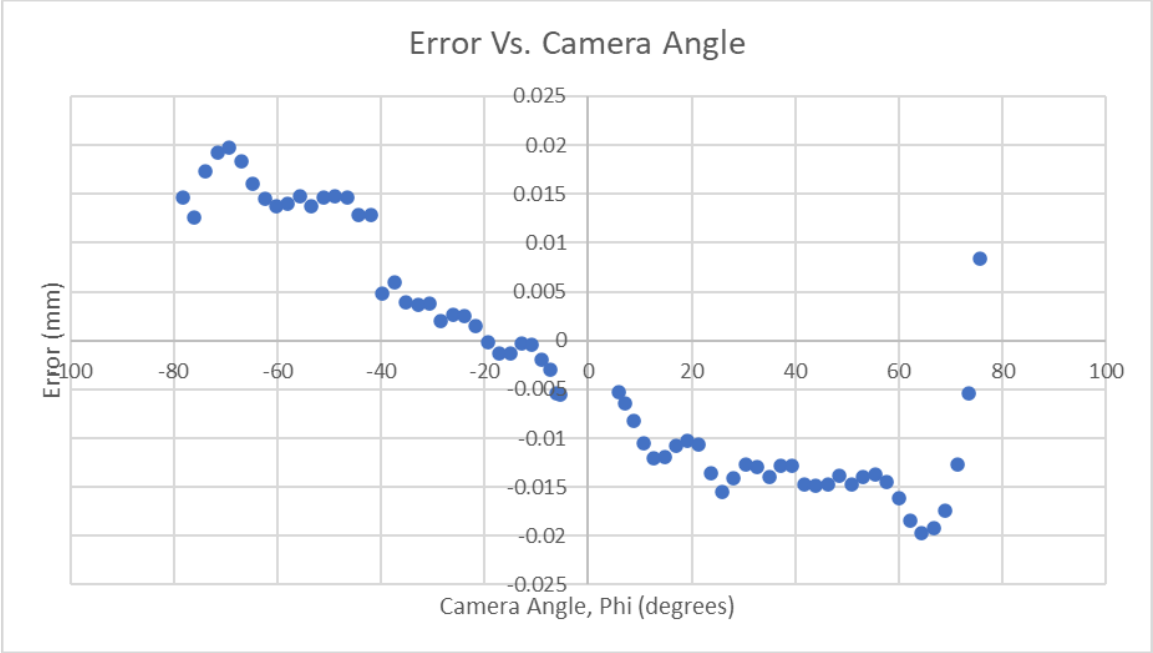


Figure 44: Camera Angle in Relation to Geometry Surface Vs. Error

Figure 44 above shows the expected relationship that the steeper the angle along the surface of the sphere becomes, the more data dropout and error is likely to occur. Note the negative nature of the angles replicates the symmetry of the sphere in relation to the scanner. Once the angle exceeds 79 degrees, the scan surface is no longer visible. Minimal error was encountered between 0 and 25 degrees on each side of the sphere, which serves to inform the angle to orient the scanner for maximizing data acquisition.

5.4 Generalized Path Plan for Scanning

The first step of automating the scanning process was the creation of a generalized path plan applicable to any geometry within the confined volume of the part positioner. In this path plan, Octopuz simulation software is used to determine the position of the scanner in relation to a geometry. The best field of view volume is implemented as a visually depicted cube in the simulation and aligned to best encompass the surface area of any part. After each segment, a wait function is implemented for the scan to commence. The path arcs along the top of the geometry to collect and store as many reference points as

possible while scanning the top surface. The collection of these reference points allows the scanner to determine the position and orientation of the part in space more easily.

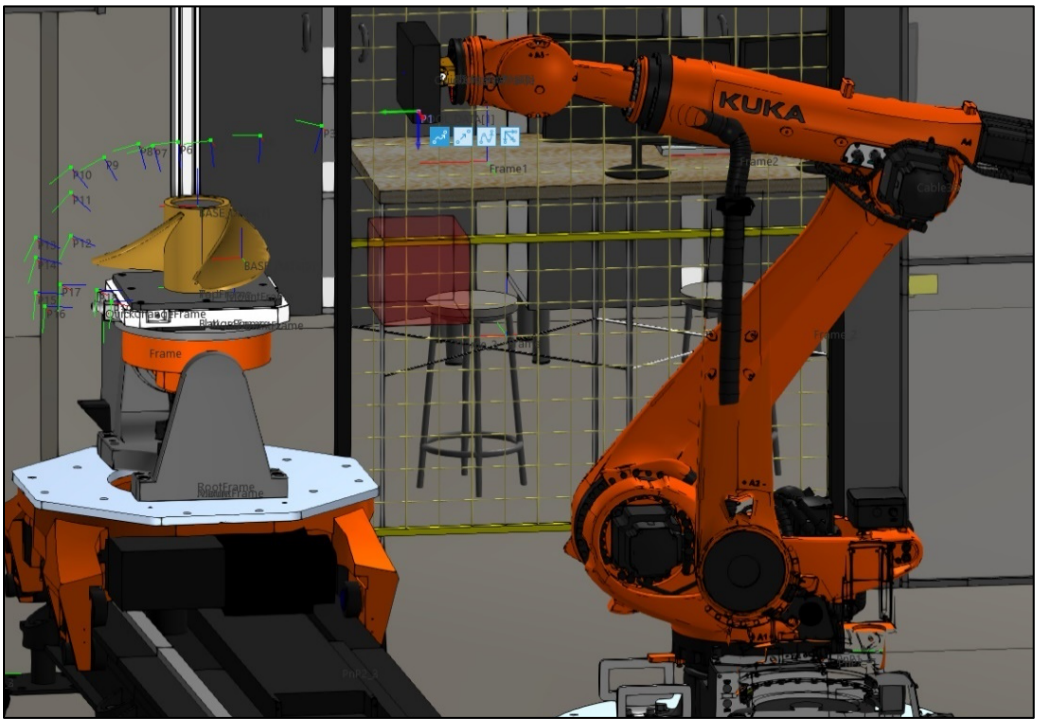


Figure 45: Generalized Path Plan

The generalized path plan administered 37 scans along the geometry. Individually, each scan using the generalized path plan requires more time due to the robot requiring time to move into position and the 30 second wait time to allow the scanner to have ample time to administer the scan between movements. The image map in Figure 46 below displays the image acquired when administering each scan from its respective position in relation to the part. The green dots are representative of the fiducials used to determine the camera position when acquiring the scans.

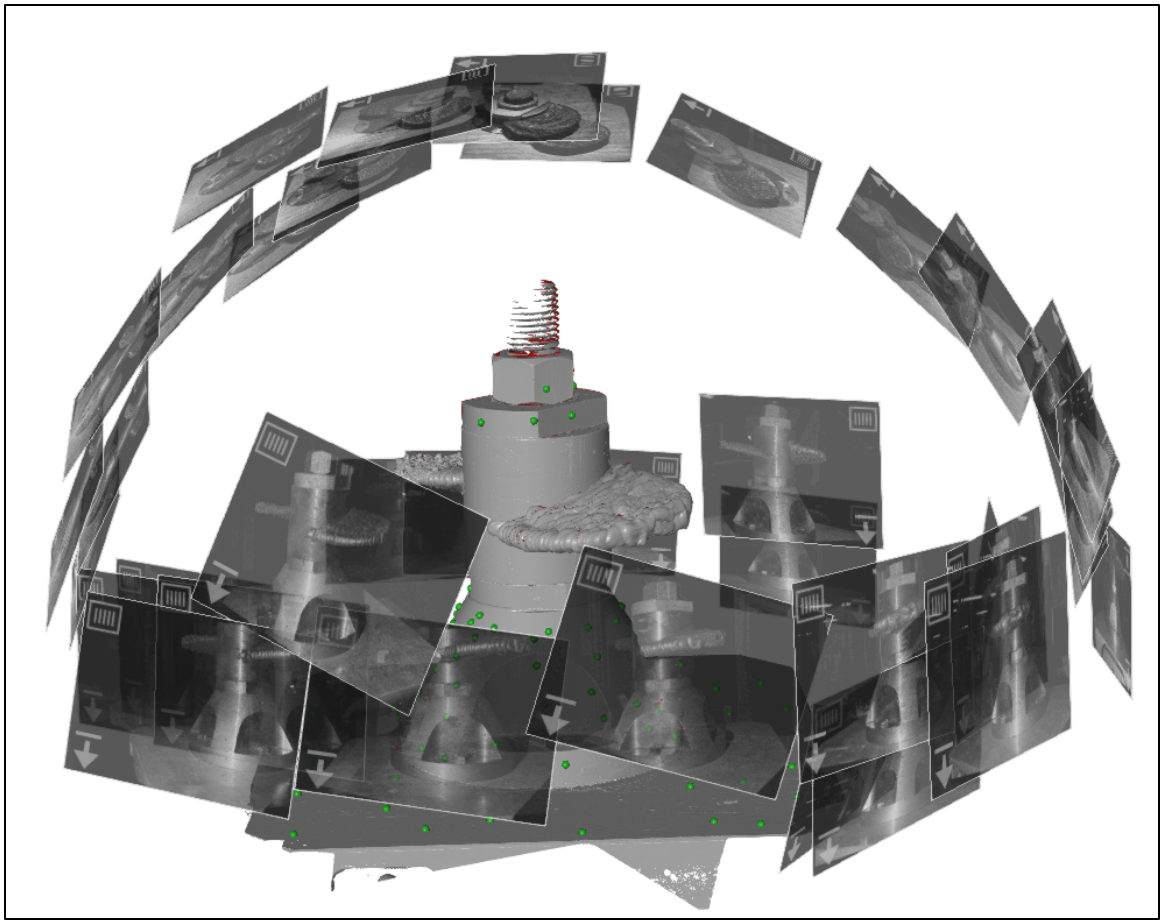


Figure 46: Generalized Scanning Path Plan Image Map

Despite the additional time allotted per scan and lack of use of the part positioner the path plan is still more efficient than traditional static scanning. The final result below was produced within 40 minutes.

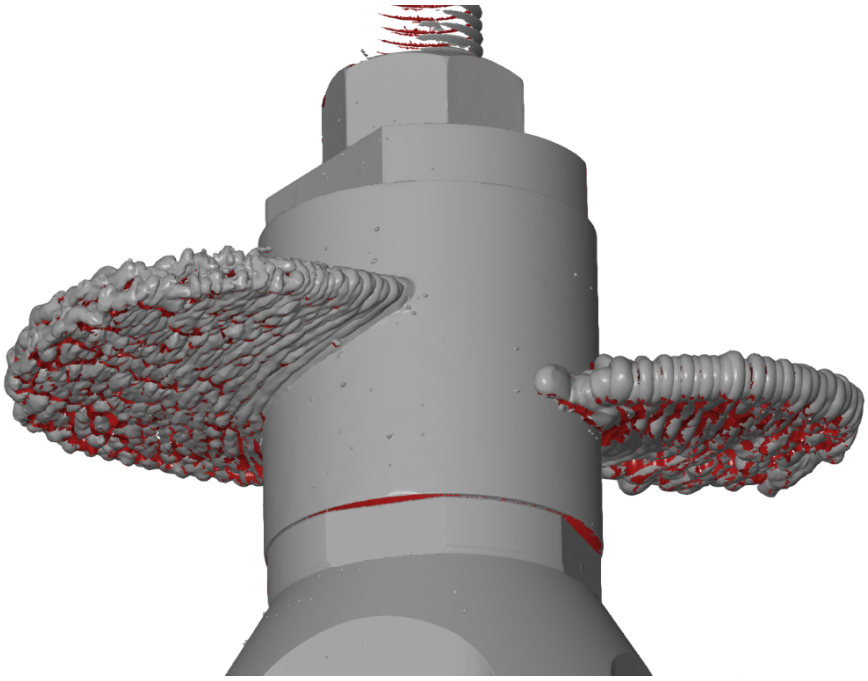


Figure 47: Result of Generalized Scanning Path Plan

The intent of this path plan was to create a versatile baseline that is applicable to any geometry and is possible to further refine as needed. It serves as a simple solution for more straightforward geometries and additions and adjustments are easily implemented for more complex geometries. The generalized path plan lays the groundwork for geometry-based path planning by providing insight into the practical application of the intended path plan, including maintaining joint axis limits as well as visibility of reference points.

5.5 Geometry Based Path Planning for Scanning

A myriad of methods were attempted in the developmental process of creating a geometry based path plan. Firstly, the center of the field of view of the scanner was defined in Octopuz robotic simulation software as a tool center point. Similar to the welding process, the tool follows along the surface geometry with wait functions at each segment to conduct the scan. Data collection from the gage ball study is used to determine ideal scanning configurations and set limiting parameters for the orientation of

the tool. The angle between the surface of the geometry and the tool are monitored and constrained to an angle of less than 50 degrees for majority of the surface, ideally mostly staying configured between 0 and 30 degrees.

5.5.1 Surfacing Function

In the first attempted method, a CAD model of the desired geometry is imported directly into Ocotpuz. The base frame is configured to position the CAD model in its proper position relative to the part positioner. The surfacing function is used to define the geometry in space, and parameters are defined for the respective camera orientation. Once desired parameters are defined, path functions are generated for the motion of camera along the surface of the geometry.

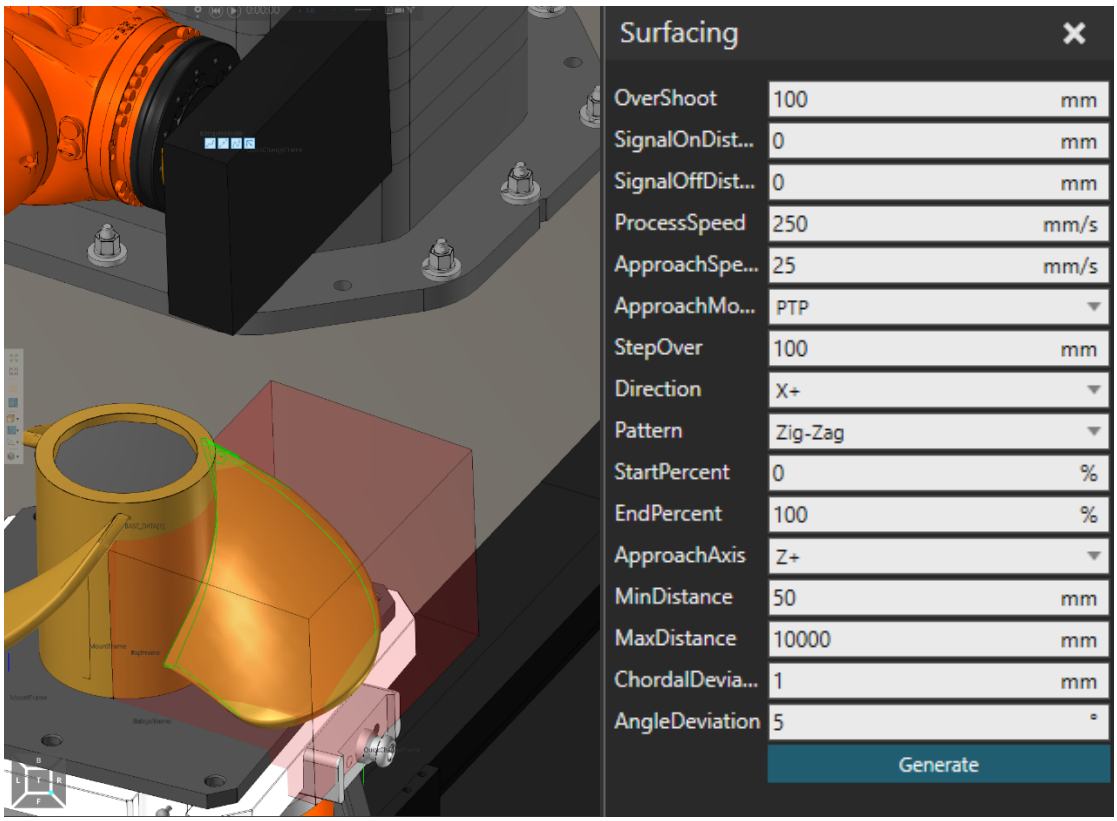


Figure 48: Surfacing Function for Path Planning

Figure 48 above demonstrates the surface selected for path planning (left) and the necessary input parameters (right) to generate the path plan. Speed, pattern, minimum distance, maximum distance, and angle deviation are the main considerations for the

intended purpose of scanning. Articulating process and approach speeds reduces the risk of wait time errors due to detected motion of the camera. The pattern setting allows adjustment for the type of pattern of the path plan motion over the geometry, additional research may be explored to determine the optimal pattern for scanning of the intended geometry.

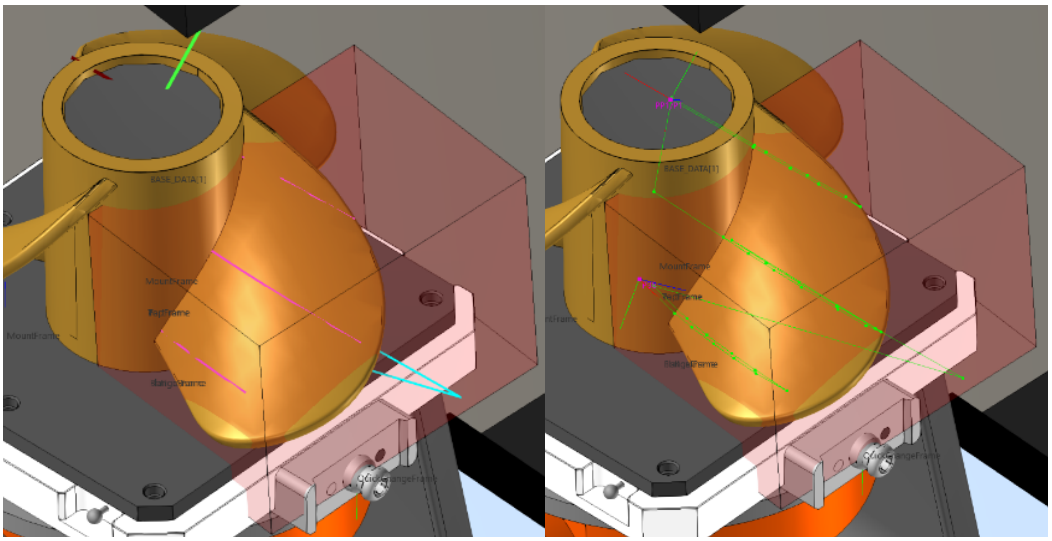


Figure 49: Surface Based Path Plan

After verification and any necessary adjustment of the paths (left Figure 49) a path plan broken into segmented points (right Figure 49) is generated for both the anterior and posterior faces of the geometry. These paths follow along the curvature of the CAD model in a gentle tool tip direction that does not exceed the angle limits. By setting the center of the field of view of the scanner as the tool center point (TCP) the geometry has a greater chance of staying within range of reference points, lower risk of collision, and the tool tip is easier to maintain the angle parameters defined in the sphere study. Wait functions are once again implemented to actuate the scanner after every motion path.

5.5.2 Utilization of the Path Planner

Another method explored was modifying the existing path planning process to accommodate scanning applications. A CAD model of the part was imported into GOM Inspect Pro for slicing and analysis. Initially, numerous slices were generated just like the printing process. This concept proved to be ineffective and cumbersome for scanning, for

there were too many paths along the surface of the part and the tool orientation was 90 degrees offset to a typical orientation of a scanner. The improper tool orientation (Figure 50) can be mitigated by changing the coordinate system of the tool as seen in Figure 51, however once the path reaches the posterior portion of the geometry, the tool must be updated point by point to avoid collision, which is an undesirable solution. For example, the path plan depicted contains 178 paths each containing hundreds of reference points, searching through and updating tool orientation as needed is impractical. It is possible to sort through the path plans individually and eliminate redundant or unnecessary paths and reference points, but this concept merely operates as a steppingstone to a long-term solution.

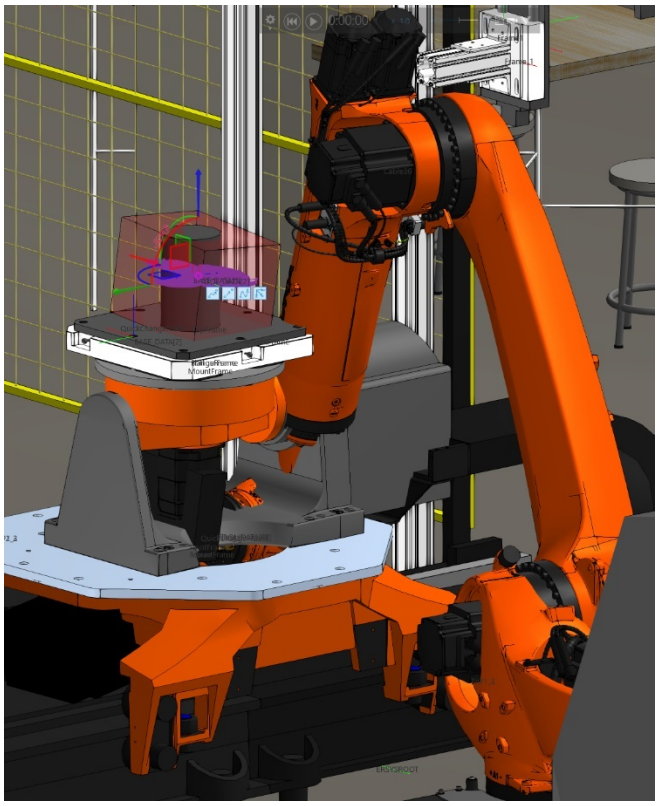


Figure 50: Imported Path Plan Orientation Collison

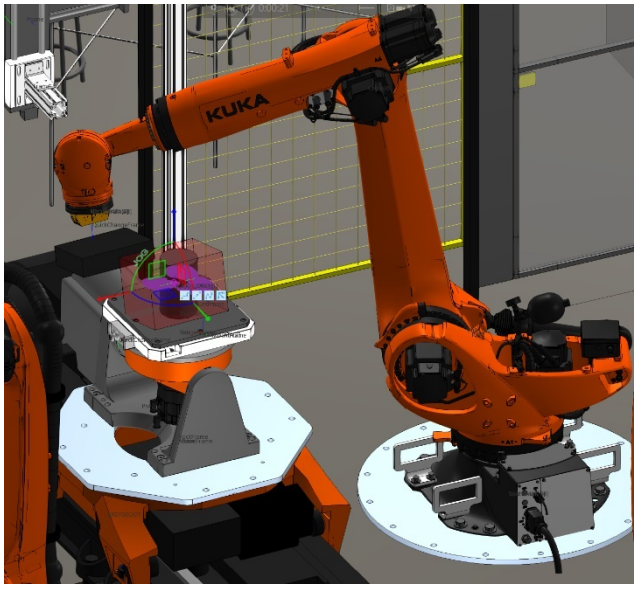


Figure 51: Imported Path Plan Orientation Adjustment

5.5.3 Refinement of the Path Planner for Scanning

With the knowledge that importing a full path plan of equal complexity to a welding path plan is too cumbersome to be practical, pursuit of a simpler solution began. Instead of starting with a full path plan and stripping it to the core, the reverse was investigated. Starting with a single slice of a desired geometry, reference points with respective nominal vectors were evenly distributed along the slice as seen below in Figure 52.

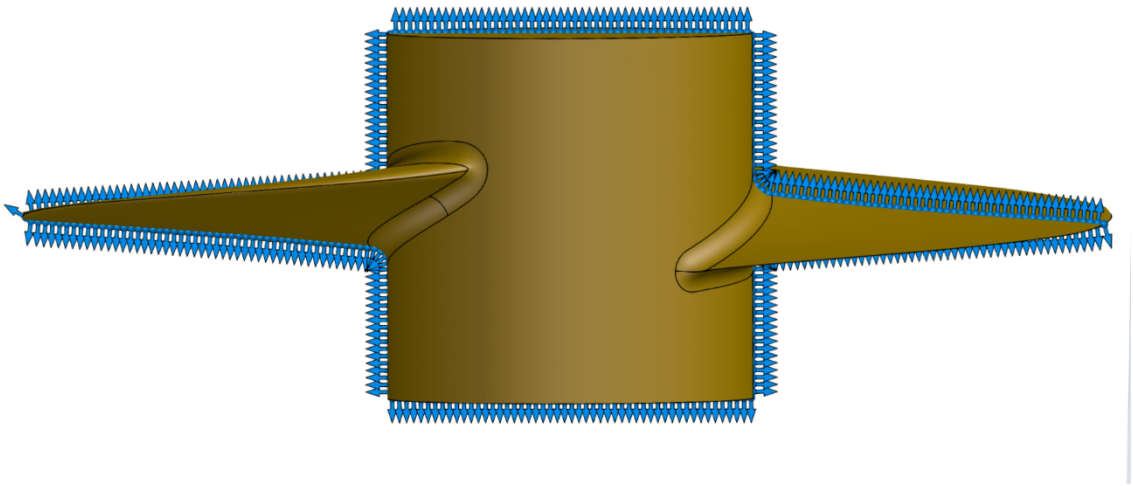


Figure 52: Surface Nominals along Desired Geometry

Systematic and visual analysis was conducted to determine areas of overlap of the nominal vectors. Overlap indicates areas of increased scanning difficulty, that encounter a higher risk of obscuration and data dropout. While extra caution must be taken with these regions of the geometry, other areas can afford a reduction in the number of scans required to produce a sufficient image. This is where knowledge from the gage ball study comes into play. Surface angles in excess of 50 degrees require additional scanning orientations, others can be diminished without significant difference in scan quality.

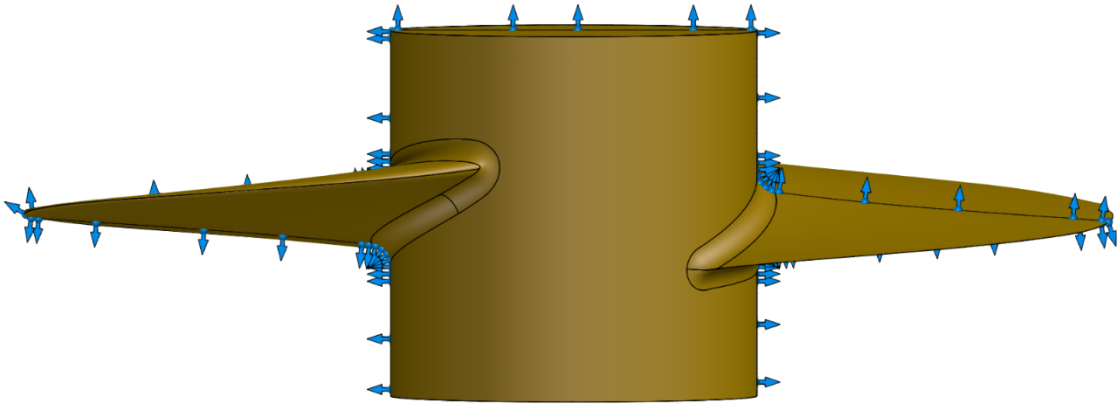


Figure 53: Nominal Vector Reduction

As seen in Figure 53 above, a significant reduction is possible to simplify the data set without sacrificing scan quality. In a similar way to the path planning process for welding, these reference points are exported as an ".ascii" file and processed the path planner for visualization (Figure 54). In this case, starting on a corner and other concerns that play a role in welding are not as applicable.

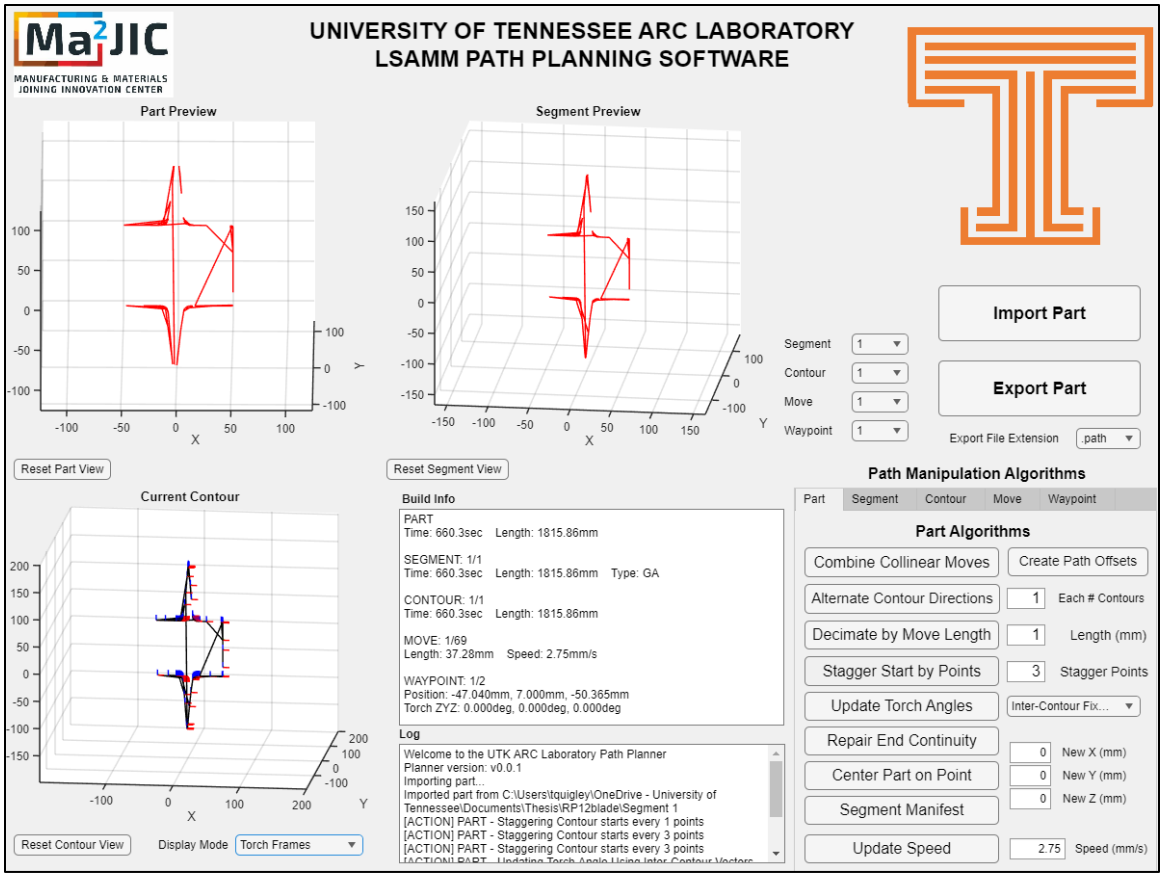


Figure 54: Scanning Path Plan

Mainly the visualization is to ensure the reference points connect effectively into a cohesive path plan. If this is successful, the reference points are processed through a tailor-made MATLAB script to update the tool angles for scanning and export as a .path file to be imported into Octopuz for simulation (Figure 55).

```
%% Import
p = FileTools.ImportPart('C:\Users\tquigley\OneDrive - University of Tennessee\Documents\Thesis\RP12blade\Segment 2');

% Decimate Moves
for i = 1:length(p.segments)

    %Combine Collinear Moves
    SegmentAlgorithms.CombineCollinearMoves(p.segments{i})
    fprintf('Decimating contours to 2mm...\n')
    SegmentAlgorithms.DecimateContoursByMoveLength(p.segments{i},2);
    fprintf('Alternating contour directions...\n')
    SegmentAlgorithms.AlternateContourDirections(p.segments{i},1);
    fprintf('Updating speed...\n')
    SegmentAlgorithms.UpdateSegmentSpeed(p.segments{i},5.08);
    fprintf('Staggering start points...\n')
    SegmentAlgorithms.StaggerSegmentStartPointsByIndices(p.segments{i},10);
    fprintf('Updating torch angles...\n')
    SegmentAlgorithms.UpdateTorchAnglesUsingInterContourVectorsWithFixedTravelPlane(p.segments{i},[0,1,0])
    fprintf('Segment %i Complete!\n',i)
    fprintf('Updating Tool Frame...\n')
    RotateSegmentPointsAboutToolFrames(p.segments{i},90,X)
end


% Create Manifest
fprintf('Creating manifest...\n')
n_segments = length(p.segments);
manifest_all_simultaneous = 1:n_segments;
PartAlgorithms.ParallelizeSegments(p,manifest_all_simultaneous);

fprintf('Saving path...\n')
file_path = 'C:\Users\tquigley\Documents\GitHub\UTK-Path-Planner\ScanPlan2_manifest.path';
PathFileWriter.WritePartWithManifest(file_path,p);
```

Figure 55: MATLAB Code for Scanning Path Plan

Once the path plan is imported into Octopuz, proper definition of tools and bases are ensured. Note the code above accommodates for the orientation depicted in the GUI. Once imported into Octopuz, the program is run and any additional adjustments to tool orientation, base data, or tool data are made. After successful refinement of the path plan in Octopuz and several simulations are deemed successful, the robot code is exported to be ran on the robot.

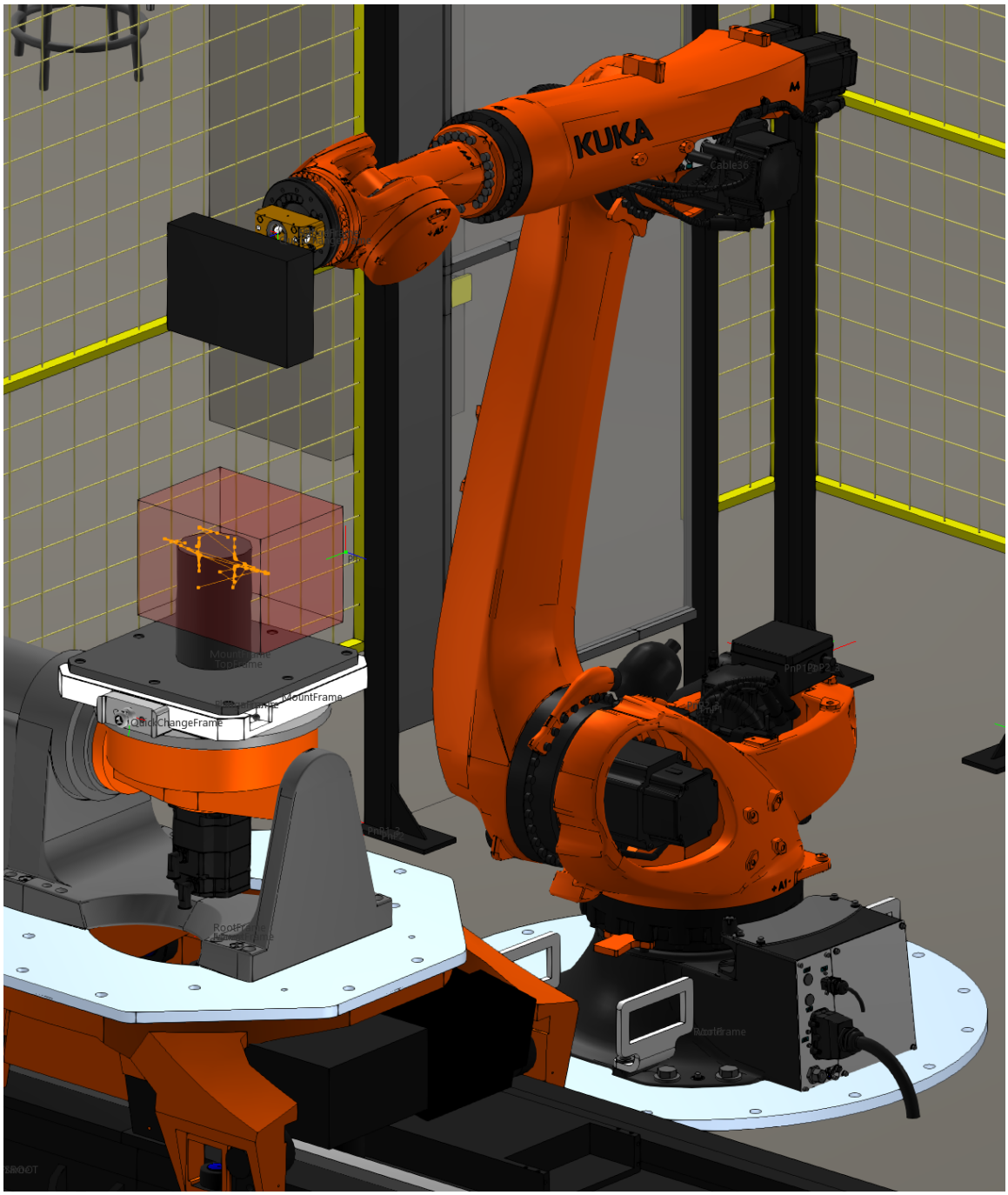


Figure 56: Geometry Based Path Plan Using Reference Points

5.6 Data Comparison/Results

An experiment was conducted to determine the quality and effectiveness of each scanning method administered. To set a control for the experiment, a printed part was

scanned by manually moving the scanner about the part until the completion of an optimal scan to the best ability of the ATOS Q scanner. The same part was then scanned via static configuration, static with a 25-degree tilt, and a generalized path plan. Each method was compared to the control via color map inspection using GOM Inspect Pro software. The color map depicts the difference in millimeters between the scans conducted. Areas of data dropout or where data isn't acquired is depicted in fuchsia pink.

5.6.1 Static Configuration Results

This section depicts the results of both a standard static mounting scan configuration as well as the implementation of a 25-degree tilt of the scanner in relation to the part. From a static configuration, 108 scans were acquired to produce a comprehensive image of the part. The image acquired was compared in relation to the previously mentioned control and the results of such are depicted in Figure 57 below.

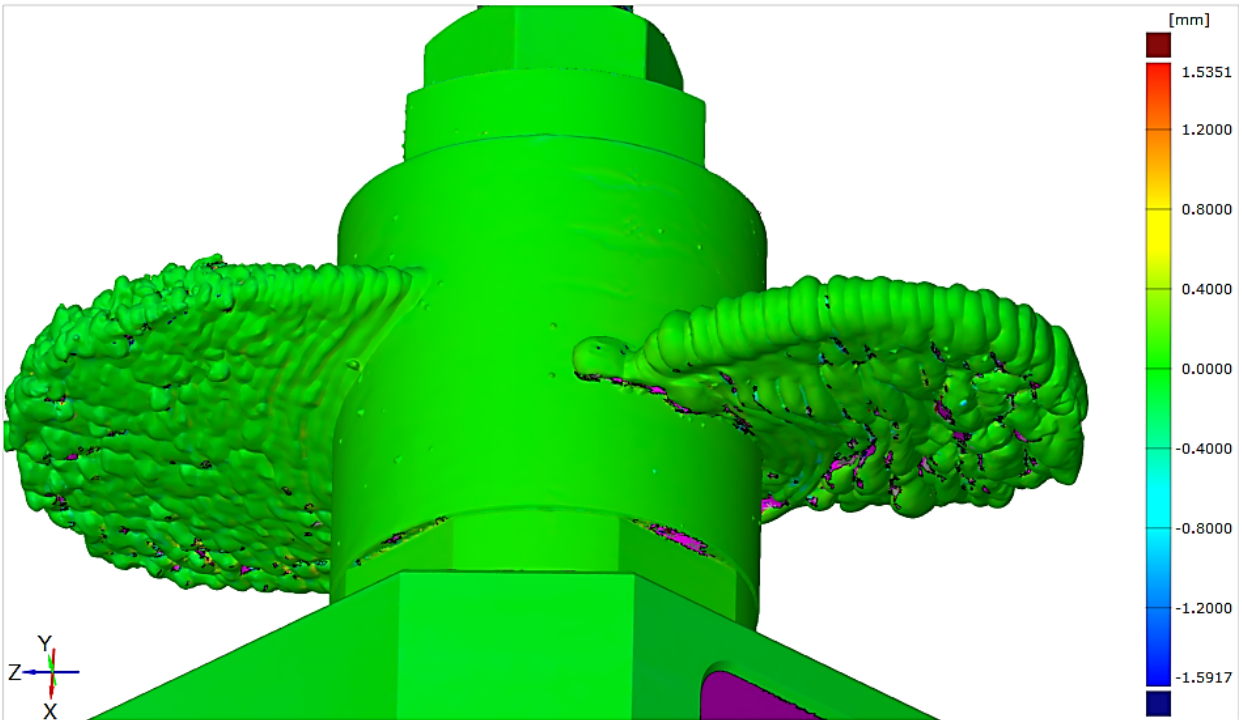


Figure 57: Static Configuration Color Map

After tilting the camera mount by 25 degrees, another set of scans were administered until an image of optimum quality was produced. In this configuration, 78 scans were

required to produce the scan analyzed in Figure 58 below. This set of scans diminishes scan time of this geometry by 35% in comparison to the static scanning method. The static configuration also increases time dramatically for the part must be tilted via the part positioner in both directions for the underside of the blades to be visible. The 25-degree configuration only requires tilt in one direction due to the angle of the camera. A deeper comparison of these results are evaluated in 5.6.3.

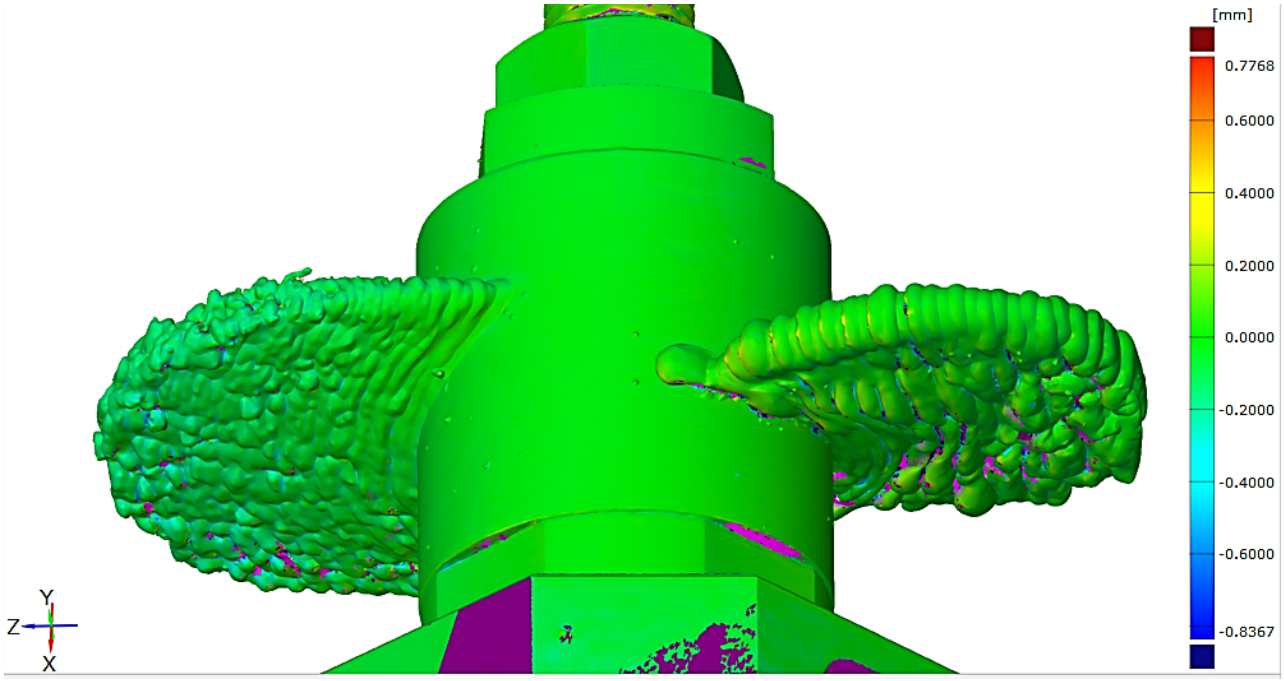


Figure 58: 25-Degree Configuration Color Map

5.6.2 Generalized Path Plan Results

Despite the near rudimentary nature of the path plan and methodology behind it, the generalized path plan generates scans of sufficient quality to machine with still greatly reducing number of scans required and thusly lead time required to scan parts of a standard size. Figure 59 and **Error! Reference source not found.** below show the error of the scans using this method in relation to the best scan of the same geometry feasible for the ATOS Q is nominal. The generalized path plan serves as a great tool when needing to machine a simple geometry or one that doesn't require in depth data differentials. The scans acquired still encounter data dropout on the posterior side of the

blade, however this is a significant improvement when considering scanning from a manual configuration.

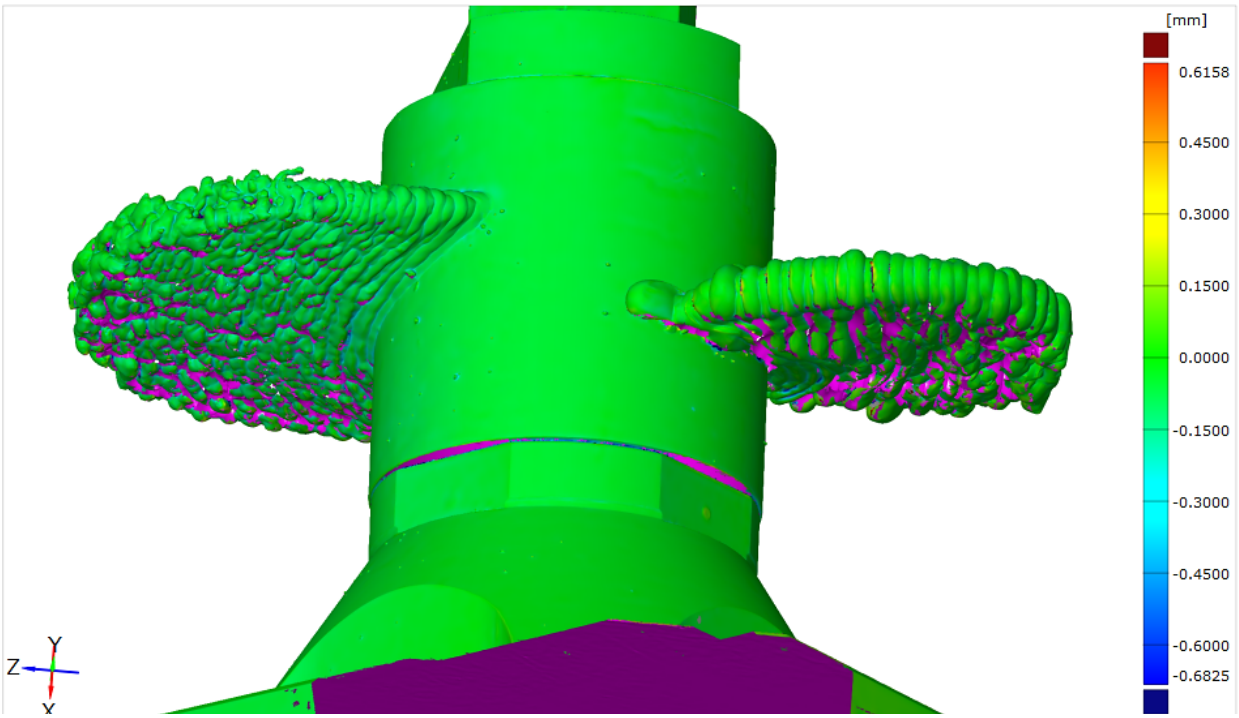


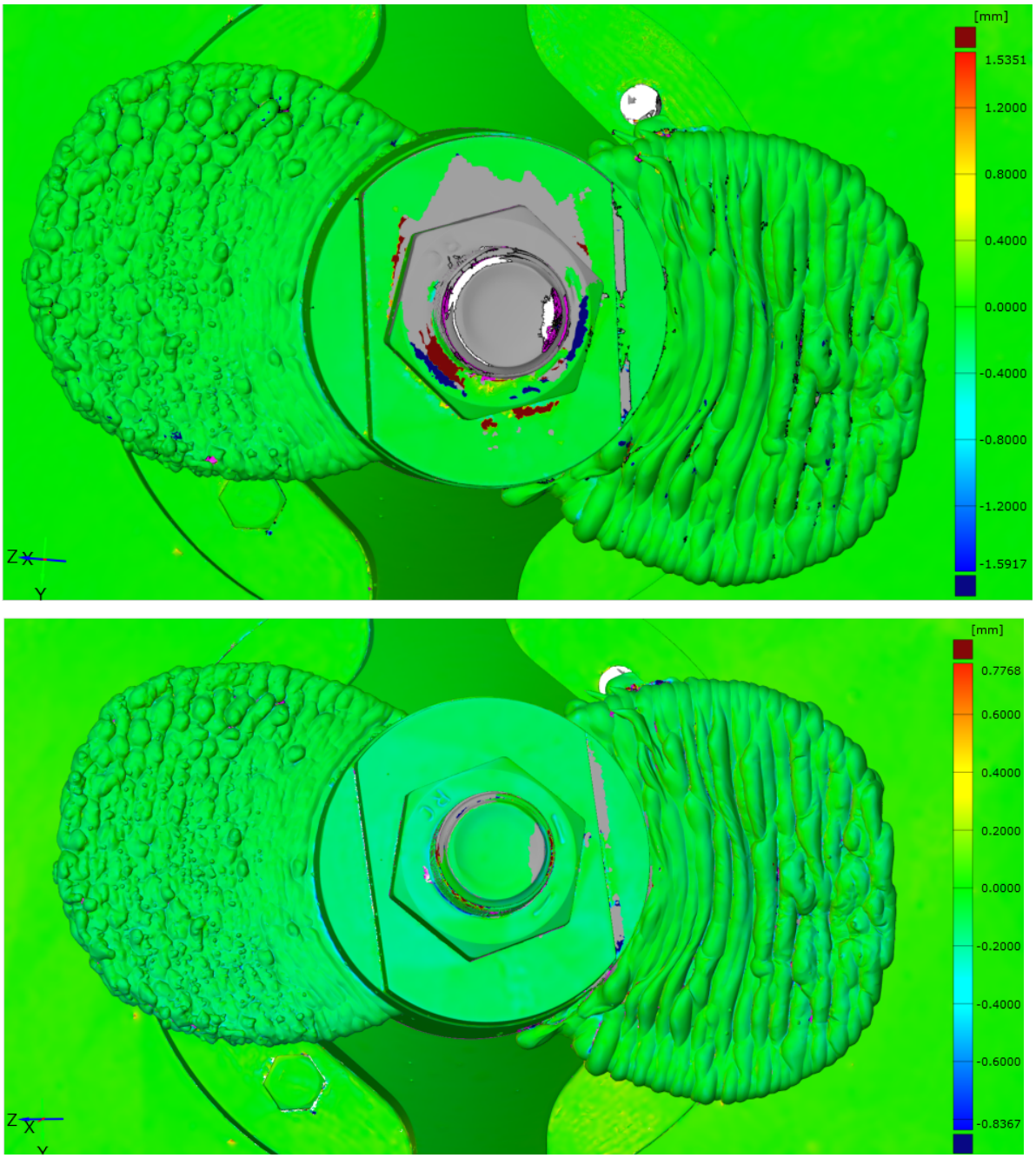
Figure 59: Color Map Comparison of Generalized Path Plan (Side View)

5.6.3 Comparisons

The following figures depict the result of each scanning method to show the progression of improvement. Each scan set is demonstrated in the same orientation for clarity.

The design of this section is to compare the results of each scanning method for quality in comparison to preeminent data collection of the geometry. Scales are depicted

accordingly along the right side of the image.



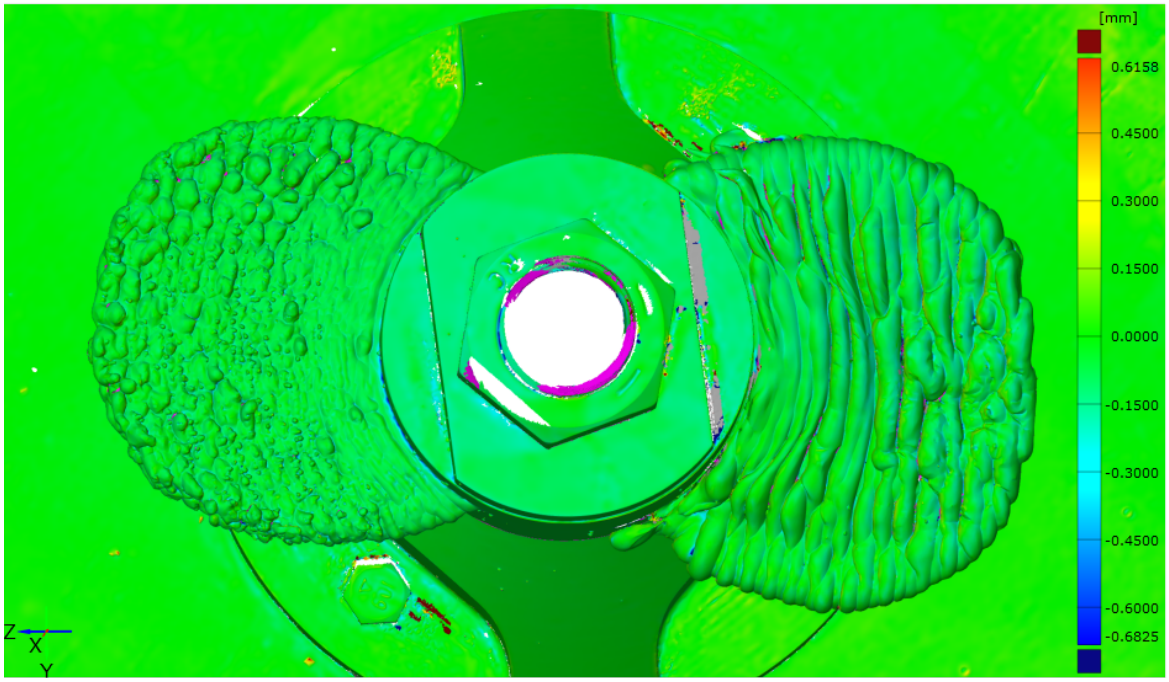
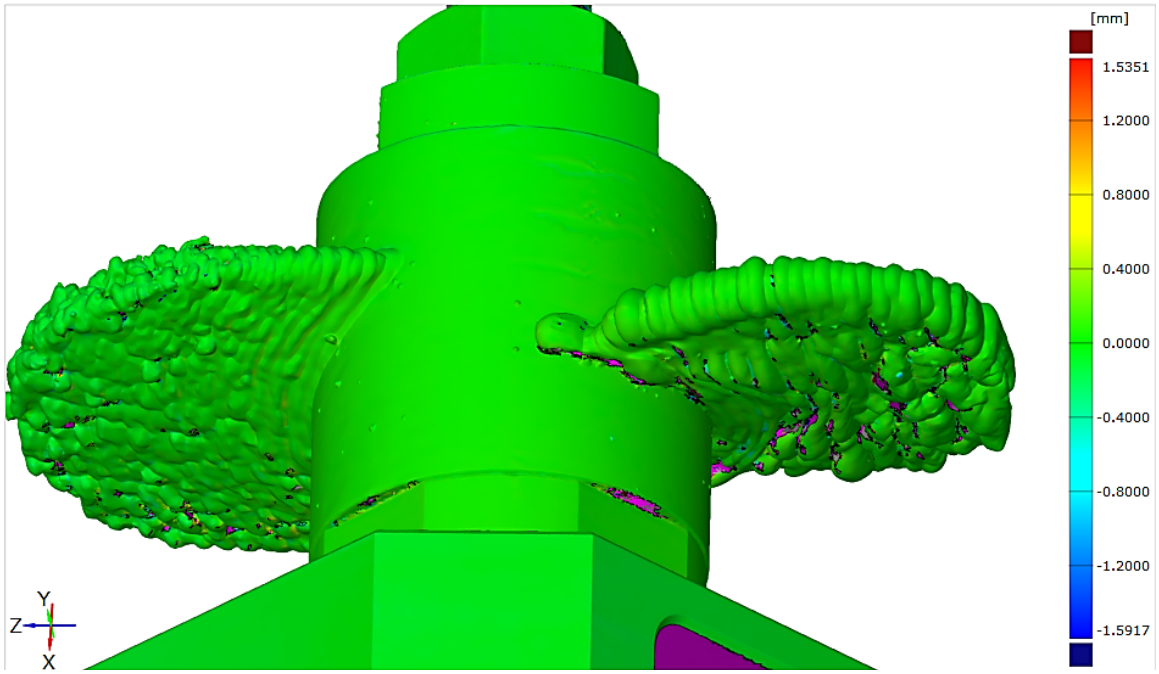
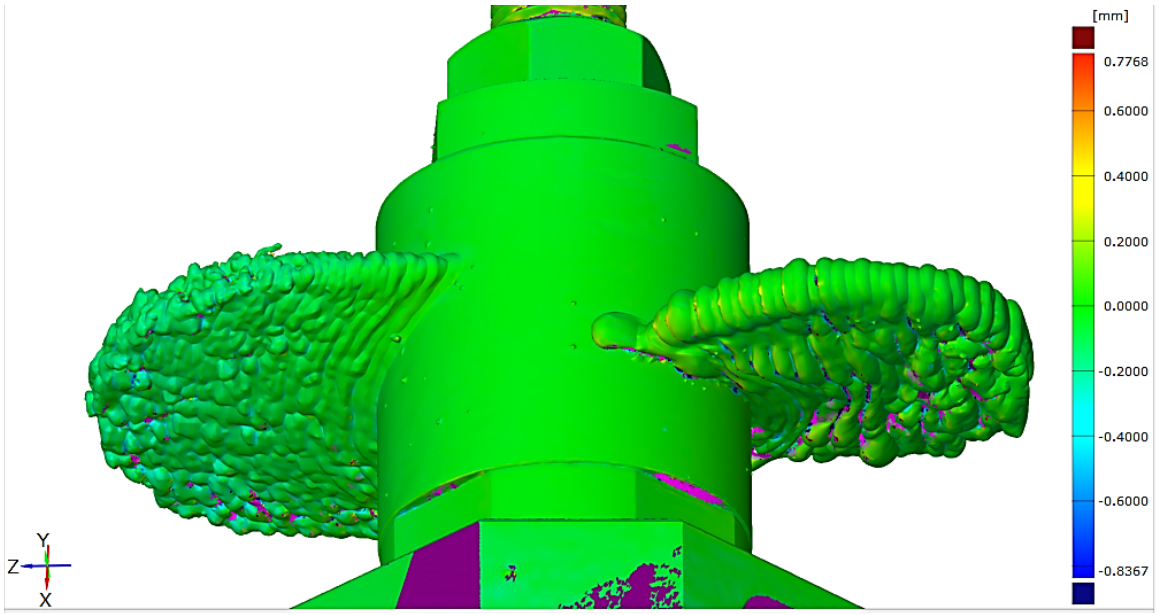


Figure 60: Data Comparison of Static Configuration, 25-Degree Configuration, and Generalized Path Plan

Table 2: Comparison of Scan Results

	Static Configuration	25-Degree Configuration	Generalized Path Plan
Number of Scans Acquired	106	78	37
Time Required	90 minutes	50 minutes	30 minutes


[mm]
1.5351
1.2000
0.8000
0.4000
0.0000
-0.4000
-0.8000
-1.2000
-1.5917
Y
Z
X


[mm]
0.7768
0.6000
0.4000
0.2000
0.0000
-0.2000
-0.4000
-0.6000
-0.8367
Y
Z
X

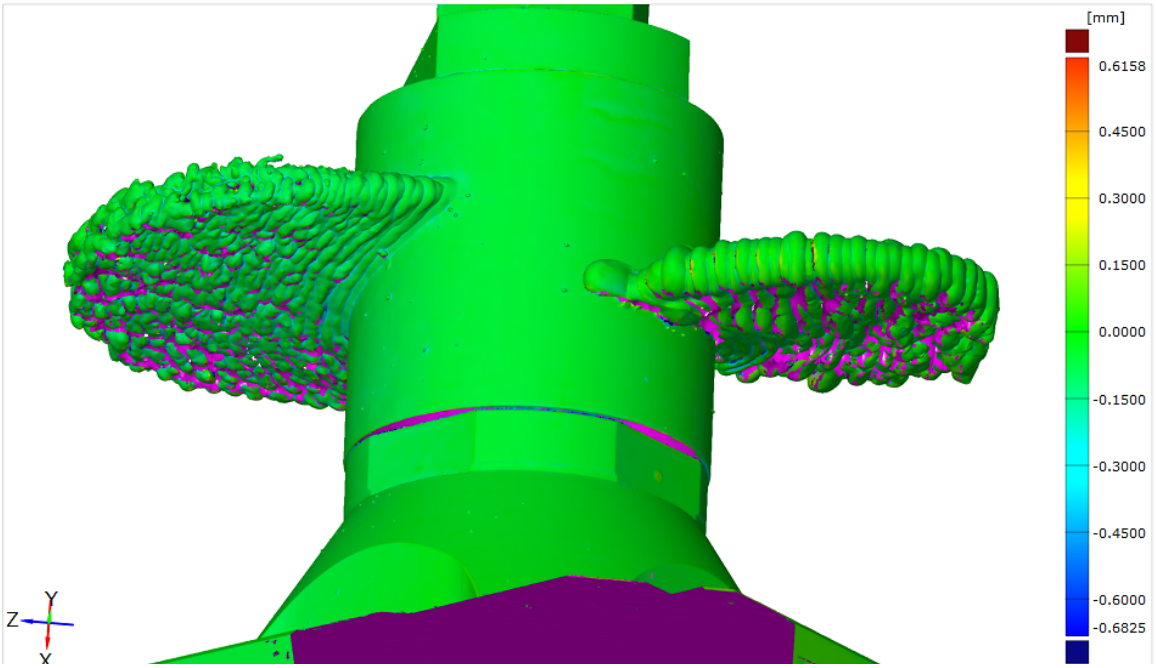


Figure 61: Comparison of Scan Results (Side View)

Setting the camera at a 25-degree angle served as a significant improvement to the static configuration by requiring nearly 45% less time with an improved scan accuracy of 47%. The generalized path plan generated scans with a 57% accuracy improvement from the static configuration and an accuracy improvement of 18% from the 25-degree configuration, while only requiring a third of the time required to administer a static configuration scan. Note despite the significant enhancement in scan accuracy, the generalized path plan did incur some significant areas of data dropout. This is to be expected, for the generalized path plan is designed to serve as a basis to further develop for a specific geometry as necessary.

5.7 Challenges

5.7.1 Transformation Error

If the camera is translated too far from its known position in relation to the part, it may administer a inability to compute transformation error. This simply means the camera lost its ability to determine its position in space. This error was greatly diminished by

implementing more fiducials especially for more complex geometries. Additionally, the scanner can be actuated again to retry the measurement. In some cases, the scan is omitted and the camera moves onto the next, which is why redundancy in scanning is emphasized.

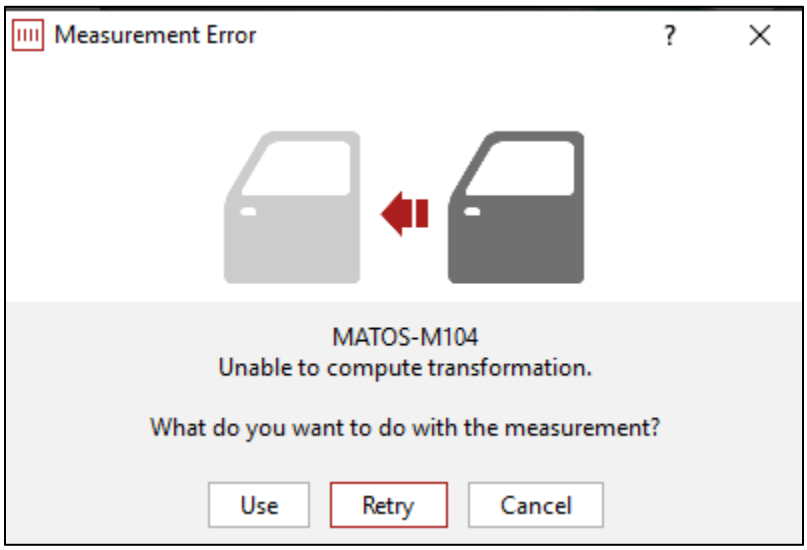


Figure 62: Transformation Error

5.7.2 Measurement Delay

If the scanner detects motion or is unable to detect enough reference points to create a reliable scan, a measurement delay is encountered. This delay can be bypassed if necessary, and in most cases is negligible due to the generous time allotted to administer each scan.

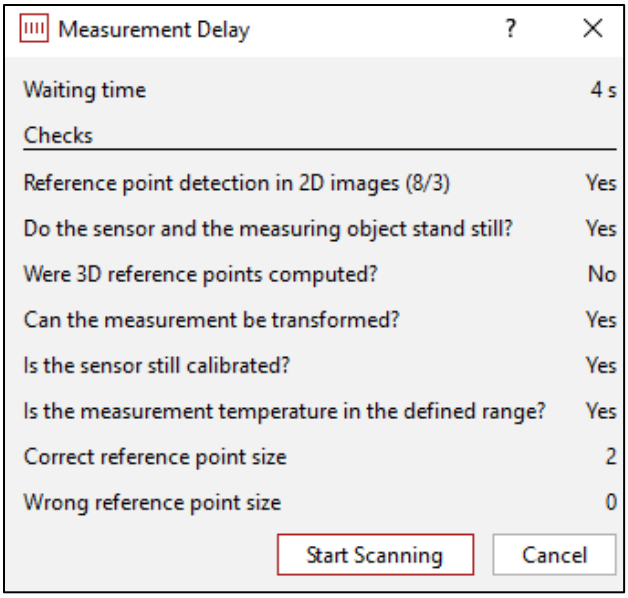


Figure 63: Measurement Delay Screen

5.7.3 Not Enough Reference Points

Another challenge of the GOM software that was faced was the inability to find enough reference points. When first mounting the GOM to the ATOS Q, this error was recurrent. It seemed the scanner would lose reference points every few scans. However, a simple solution that mitigated this issue was the simple addition of more scanning fiducials to the base of the part. This made translations of greater magnitude much easier to stay within range of the required 3 visible reference points.

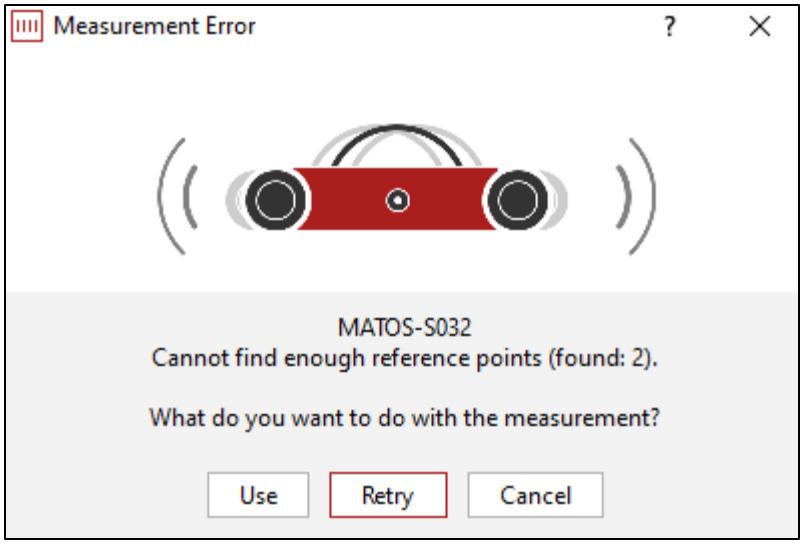


Figure 64: Insufficient Reference Points Error

Chapter 6

Conclusions And Recommendations

6.1 Conclusions

Path planning with degree of freedom redundancy is successfully conducted utilizing the KPL3. Where possible, gravity alignment is achieved and maintained for WAAM prints of simple to complex geometries. Similar path planning techniques were used to create a path plan for metrology antiquated for the respective geometry. Starting from improving upon a static configuration of scanning, the scanner was mounted to the KR250 robotic manipulator and was found to efficiently produce quality images. This process was further refined to a path plan that acquired sufficient images for the informed machining process in significantly less time without dramatic sacrifice to quality of data acquired. Further refined, a variety of theories were explored in determining the feasibility of creating a geometry-based path plan. The plan performed with great success on simulations and the KRL code was able to be exported for execution on the robot.

6.2 Recommendations

6.2.1 Implementation of Algorithm

When implementing the geometry-based path plan, the current method is to analytically determine the reference points and orientations to utilize. To move toward automation and diminish lead time on generating a geometry-based path plan, future work would include creating an algorithm to determine which reference points to reduce and which to maintain. This algorithm would ideally select reference points on the premise of degrees of convex/concave curvature of the surface. As informed via the gage ball study, the camera would maintain an angle between 0-30 degrees relative to the surface of the geometry. Along a convex surface, this may be considerably more difficult to maintain as

seen in the underside curvature of the propeller blade, leading to deposition of multiple reference points in regions necessary. Ideally, the algorithm would apply an informed orientation angle constraint of 0-30 degrees as well as implement multiple scan configurations in areas of concave curvature to ensure adequate scan data acquisition.

6.2.2 Coupling of the KR250

In future work, it would significantly improve the quality and efficiency of scans if the part positioner was viable for use in this process. A current limitation of the hybrid manufacturing cell is the part positioner can only be coupled to the KR50 robotic manipulator, used for WAAM. The two can be coupled via hardwiring for the KR50 has an additional servo amplifier designed for this very purpose. The servo amplifier serves to support the motors within the KR50 and the additional is used for the part positioner. Contrarily, the KR250 only has the amount of servo amplifiers required for its solidary motion. An idea to overcome this issue was to hardwire the KR250 to the KR50 to use the additional servo amplifier to run the part positioner. However, this idea was never explored due to the risks outweighing the potential likelihood of success of this circumvention. For one, all of the robots used in the hybrid cell are taught as one project in Work Visual, a software developed by the manufacturer for the purposes of integrating multiple units into one system. Presently, one project is necessary for all aspects of the hybrid cell including welding and scanning. If the KR250 was hardwired to the KR50 to bypass the servo amplifier limitation for the purposes of coupling the part positioner, an entire new project would need to be created for the new system. The two projects would be unable to run simultaneously, so the original project would need to be retaught when changing back to the original system configuration. Another potential risk would be feedback being communicated to the wrong place; this could lead to conflicting messages of the system between its components leading to unpredictable executions from the robots. Roboteam is a tool with potential to mitigate this issue. Instead of operating off hardwiring the units to one other, it is a network-based software. It operates off the same premise as ethernet KRL (Kuka Robot Language) which transcribes motion and speed to each robot.

Bibliography

Du, H., Chen, X., Xi, J., Yu, C., & Zhao, B. (2017). Development and Verification of a Novel Robot-Integrated Fringe Projection 3D Scanning System for Large-Scale Metrology. *Sensors, 17*(12), 17, 2886.

KUKA Robotics. (2017). COnfiguration of Kinematic Systems V2 For KUKA System Software 8.5 Assembly and Operating Instructions. Ausburg, Germany: KUKA Robotics.

Products: ATOS Q. (2022, June). (Ziess GOM Metrology) Retrieved 2022, from https://www.gom.com/en/products/3d-scanning/atos-q

Tan, D. L. (2015). Experimental Investigation of the Role of Large Scale Cavitating Vortical Structures in Performance Breakdown of an Axial Waterjet Pump. *Journal of Fluids Engineering*, 137(11), 1.

Triangulation: proven measuring principle with a future. (2022, March). (Ziess GOM Metrology) Retrieved 2022, from https://www.gom.com/en/topics/triangulation

Vals, E. C. (2022). *"Redundant Kinematics Solution for a Combined 6DOF Robotic Manipulator and 2DOF Part Positioner in a WAAM Application. "* . Retrieved from University of Tennessee: https://trace.tennessee.edu/utk_gradthes/6429

Vita

Originally from Tennessee, Tiffany Quigley attended Florida Institute of Technology and received a Bachelor of Science in Aerospace Engineering with a minor in Flight Technology. After graduation, she decided to pursue a Master of Science degree in Aerospace Engineering with a research concentration of Robotics where she had the fortunate opportunity to kinesthetically research robotic manipulators and controls in additive manufacturing and metrology applications. She is greatly appreciative towards all who supported her in achieving this goal. After graduation she will begin commercial airline pilot training and studying to apply for a fighter pilot position in the Air National Guard in pursuit of her dream of becoming an astronaut.